MOTION OF A CHARGED PARTICLE IN THE GRAVITATIONAL AND MAGNETIC FIELD OF A PULSAR

MOTION OF A CHARGED PARTICLE IN THE GRAVITATIONAL AND MAGNETIC FIELD OF A PULSAR

BY

KHALID SAIFULLAH

SUPERVISED BY

PROFESSOR ASGHAR QADIR

DEPARTMENT OF MATHEMATICS

QUAID-I-AZAM UNIVERSITY

ISLAMABAD PAKISTAN

1992

MOTION OF A CHARGED PARTICLE IN THE GRAVITATIONAL AND MAGNETIC FIELD OF A PULSAR

By
KHALID SAIFULLAH

A dissertation submitted
in partial fulfillment of the requirements
for the degree of
MASTER OF PHILOSOPHY
in
MATHEMATICS

DEPARTMENT OF MATHEMATICS
QUAID-I-AZAM UNIVERSITY
ISLAMABAD
1992

CERTIFICATE

We certify that we have read this dissertation and that in our opinion it is fully adequate, in scope and quality, as a dissertation for the degree of **Master of Philosophy**.

____

(Chairman and Supervisor)

____

(External Examiner)

To ammi and abbu

The pulsar's Pindar

DIETRICK E THOMSEN and JONATHAN EBERHART

From Science News 93 (15 June 1968)

[This poem has been dedicated to S Jocelyn Bell of the Cambridge University Mullard Radio Astronomy Observatory, 'whose persistence led astronomy's most awesome personages to the pulsar's puzzling performance. It was written by Dietrick E Thomsen and Jonathan Eberhart in 1968, in the early days of pulsar investigation, when the nature of these heavenly bodies was very mysterious, and the number of them known was only four.]

Rhythmically pulsating radio source,
Can you not tell us what terrible force
Renders your density all so immense
To account for your signal so sharp and intense?

Are you so dense that no matter you own;
No atoms nor protons, save neutrons alone?
And do you then fluctuate once every second
So fixed that by you all our clocks might be reckoned?

Or are you two stars bound together in action
That spin like a lighthouse beam gone to distraction?
What in the world can account for your course
O rhythmically pulsating radio source?

And perhaps is there more than your radio beam?
Perhaps visible light in a radiant stream?
And what if the cause of your well-metered twitch
Is a strange but intelligent hand at the switch?

A world of astronomers ponder, a-pacing,
The cause of your infernal, rock-steady spacing,
To see your pulse vary, they valiantly strive,
From 1.3372795.

But the biggest of mysteries plaguing our earth
Is, how of your kind can there be such a dearth?
In infinite space one should find ever more;
Can it be that your number indeed is but four?

PREFATORY NOTE

Astrophysics is an exciting and rapidly advancing field of research on theoretical, observational and experimental fronts. The discovery of radio pulsars in 1967 by the group of Cambridge astronomers led by Antony Hewish ranks among the most important and influential observations in modern astrophysics. The Swedish Academy of Sciences recognised the work that culminated in the discovery of pulsars by awarding Hewish the 1974 Nobel Prize in physics.

The impact of the discovery on the international science community was enormous. Within a few weeks most of the larger radio telescopes in the world were directed toward the newly discovered object. Astronomers put their efforts toward detecting additional pulsars. Astrophysicists directed their efforts toward understanding the clock mechanism. In 1968 alone more than 100 papers reporting observations of pulsars or their interpretation were published.

Pulsars were a new source of cosmic rays and they provided a new method of estimating distances on cosmic scales. Also, the existence of gravitational waves, as described by Einstein's theory of general relativity, gets its strongest support from the observations of a binary system containing the pulsar PSR 1913+16.

Although the rotating neutron star model of T. Gold now provides a well established basic frame work for pulsars, many theoretical aspects, particularly the electrodynamics of pulsar magnetospheres and the explosion mechanism of supernovae that give birth to neutron stars are still evolving rapidly. The supernova explosion of 1987 provided the researchers with an opportunity to have a 'closer' look at the mechanism.

At the time of birth the pulsars are imparted high velocities, of the order of hundreds of kilometres per second; the Vela pulsar, for instance, is off the centre of the Vela nebula. This phenomenon is known as pulsar drift. It has been suggested that the force responsible for the catastrophic event is asymmetric and depends on a high angular momentum of the rotating sources. The suggestion relies on an electromagnetic mechanism appealing to the behaviour of charged particles in the plasma surrounding the source. It is consequently very important to study exactly the motion of these charges in the strong gravitational and magnetic fields one comes across in the case of rotating neutron stars. This motion is studied in the last chapter of this dissertation. In chapter 3 the basic observational properties of pulsars are given and their models discussed. The theory of compact objects required to study the pulsar models, and stellar structure and evolution in general are discussed in the second and the first chapters respectively.

I don't have words to thank my teacher and supervisor Prof. Asghar Qadir whose teaching first inspired my serious interest in Mathematics, in general, and Relativity, in particular. I am greatly indebted to my co-supervisor Dr. Khalid Rashid, to Mr. Abdul Wasim Siddiqui, Dr. (Maj.) Mohammad Rafique, Dr. Saifuddin, Mr. Amjad Pervez and Mr. Hamid Saleem for some valuable discussions and help in computational work.

My particular thanks are also due to Mr. Anjum Latif and my brother Tariq Abaidullah who helped me in preparing the figures.

May 1992 *K. Saifullah*

CONTENTS

1

STELLAR STRUCTURE AND EVOLUTION

Through all the ages the stars have run their courses uninfluenced by man, who has always wandered about these celestial spheres. Their wanderings have, over the course of the ages, crystalized into a physical theory. Today much of the universe is interpreted on the basis of our ideas regarding the nature of stars and their evolution. It seems that all of astrophysics, ranging in proximity from the earth and its environs to the farthest reaches of the observable universe, is moderated in part by our conception of a star. An outline of these relationships is indicated schematically in Figure 1.1. The many scientific speacialities that are related to the various functions of stars are evident there.

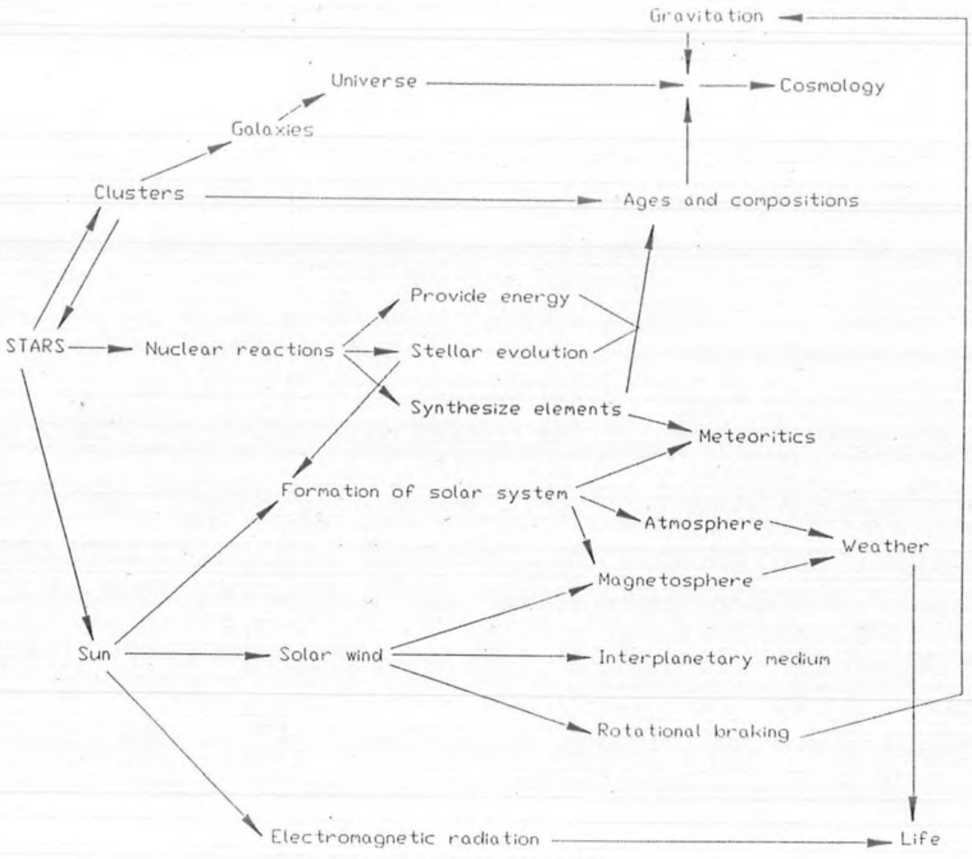

Fig. 1.1. The role of the star in astrophysics. Almost every subject in astrophysics and space science is influenced by our conception of the structure and evolution of the stars. (Taken from *Principles of Stellar Evolution and Nucleosynthesis* by Donald D. Clayton.)

1.1 STARS

A star is a self-gravitating ball of gas radiating energy into space. This energy is produced mainly by thermonuclear reactions taking place in the deep interior, but some energy may also be released during contraction or collapse of the stellar core. The star must produce energy in order to maintain enough internal pressure to support itself against its own gravitational field. Stellar structure and evolution are controlled by these two opposing effects: gravity, which tends to collapse the star, and pressure, which tends to expand it. Sometimes one or the other wins slightly, and the star may expand or contract, but there is no doubt which will win in the end. Gravitational collapse must ultimately turn the star into a cold, dead object, like the white dwarf companion to Sirius, or perhaps into a neutron star, like the pulsar in the Crab nebula, or possibly into a black hole. It may also set off the explosive event we call a supernova. Gravitation is also responsible for the initial formation of stars out of protostellar material. As soon as a large enough mass of this material becomes detached from its surroundings, it begins to contract, and one or more stars may form from it. Gravitation is the dominant creative force in the universe, and, because of gravitational collapse, it is the dominant destructive force as well.

1.2 LUMINOSITIES, MASSES, AND RADII OF STARS

The parameters conventionally adopted for the specification of the physical properties of a star are the luminosity L (normally taken to be the total rate of loss of energy by radiation from the stellar surface), the mass M and the radius R. Values of these parameters can often be determined empirically or semi-empirically. Since stars do not have a constant temperature, nor is it possible to go and measure the temperature directly, there is a problem of how to define the temperature of a star. All that we can base it on is the observed energy radiation from the star. From L and R follows the *effective temperature* T_e , which is *defined* (using the Stefan-Boltzmann law) by the relation

$$T_e^4 = L \;/\; 4\Pi R^2 \sigma \ , \tag{1.1}$$

where σ is Stefan's constant. For the sun we have

$$L_\odot = 3.90 \times 10^{33} \ \text{erg/sec.}$$

$$M_\odot = 1.989 \times 10^{33} \ \text{gm.}$$

$R_\odot = 6.960 \times 10^{10}$ cm.

$T_e = 5800$ K.

Solar units are frequently used for L, M and R. These three parameters show a tremendous range of values for the various stars. Taking extreme limits we have [1]

$10^{-6} L_\odot \leq L \leq 10^6 L_\odot$ (factor of ~ 10^{12} in L);

$(1/800) R_\odot \leq R \leq 1500 R_\odot$ (factor of ~ 10^6 in R);

$(1/20) M_\odot \leq M \leq 50 M_\odot$ (factor of ~ 10^3 in M);

$2000 \text{ K} \leq T_e \leq 100{,}000$ K (factor of ~ 50 ($\approx 10^{1.7}$) in T_e).

In terms of the language of magnitudes, the luminosity is measured by the quantity called the absolute bolometric magnitude, which is the absolute magnitude the star would have if the detector were able to respond to its entire radiant spectrum. To obtain the total energy radiated from a star requires making what is called a *bolometric correction*. The bolometric correction adds to the received energy from the star that amount of energy which is believed to be absorbed in the earth's atmosphere or is otherwise unmeasured by the detector. If the bolometric correction is designated by BC and the absolute visual magnitude by M_w, then the absolute bolometric magnitude is defined by

$$M_b = M_w + BC \ . \tag{1.2}$$

Expressing the luminosity in units of the luminosity of the sun we get

$$M_b = -2.5 \log(L/L_{\odot}) + 4.72 \ , \tag{1.3}$$

where the absolute bolometric magnitude of the sun is +4.72.

1.3 CHEMICAL ABUNDANCES

It was not until the 1920s that atomic theory and excitation and ionization conditions were sufficiently well understood that accurate abundance analyses could be made. Important investigations were made by A.Unsöld, H.N.Russell, and others. In 1929 Russell found abundances for a large number of elements in the sun.

A tremendous number of stellar composition investigations have been carried out since then. For the more or less normal stars, all but a small percentage of the mass is hydrogen and helium. The H/He ratio is probably between 3/2 and 3/1 by mass. The heavier elements are mostly carbon, nitrogen, oxygen, and neon, with very small amounts of the 'metals', such as silicon, iron, sodium, potassium, and calcium, and just traces of the other elements.

1.4 CLASSIFICATION OF STELLAR SPECTRA

There are many different kinds of stars in the sky. Most of the stars that we can see on a clear night are very similar to the sun. But there are other kinds of stars. For example, almost every reddish-coloured star we see in the night sky is a red giant. Antares in Scorpius, Arcturus in Boötes, and Betelgeuse in Orion are typical red giant stars.

One of the earliest results of observational astronomy was the realization that there existed a correlation between properties of the stellar surface, such as its surface temperature, and the strength of specific absorption lines as seen in the spectrum of the star. An empirical classification scheme was subsequently developed in which stars were sorted into principal spectral types, each type being characterized by a certain range of surface temperature and the appearance of characteristic absorption lines. The sequence of spectral classes, after many modifications and simplifications, can be given as

```
                                  S
                                /
O —— B —— A —— F —— G —— K —— M     ;
                          \
                            R —— N

      blue         yellow        red
```

(mnemonic device: Oh Be A Fine Girl Kiss Me Right Now, Smack). Each of these major divisions or classes is further subdivided into 10 groups. For instance, the spectral type B is further subdivided into 10 subclasses labelled B0, B1, B2,..., B9, in order of decreasing tempperature. Some characteristics of these classes are given in Table 1.1.

1.5 THE HERTZSPRUNG-RUSSELL DIAGRAM

The fundamental correlation between observable stellar properties was initiated by the Danish astronomer E.Hertzsprung in 1911, when he plotted the apparent magnitude of stars within a given star cluster against their colours. The American astronomer H.N.Russell made a similar investigation of the absolute magnitude of stars in the solar neighbourhood in 1913. The *Hertzsprung- Russell diagram* or simply H-R diagram, is the name given to the

Type	Temp.(K)	Colour	Typical Star	Remarks
O	50,000	Greenish white	Zeta Puppis	Helium prominent
B	28,000	Bluish	Spica	Helium prominent
A	10,700	White	Sirius	Hydrogen lines prominent
F	7,500	Yellowish	Beta Cassiopeiae	Calcium lines prominent
G	6,000	Yellow	The Sun	Metallic lines very numerous
K	5,000	Orange	Arcturus	Hydrocarbon bands
M	3,400	Orange-red	Wolf 359	TiO bands developing strongly
R,N	3,000	Red	U Cygni	Strong CN, CH, C_2 bands; TiO absent
S	2,600	Red	R Andromedae	Strong ZrO, YO, LaO bands.

Table 1.1. Classification of stellar spectra.

graph of a quantity that measures the luminosities of stars (luminosity, absolute bolometric magnitude, apparent visual magnitude, etc.) versus the effective surface temperature (or spectral class or colour index B-V, B being the blue magnitude, V the visual magnitude). It is one of the most valuable correlations established in observational astronomy.

When such a diagram has been constructed for a large number of observable stars, it is clear that a very large percentage of the stars fall on a heavy diagonal curve, called the *main sequence*, see Figure 1.2. This curve is such that the brightest objects in the sky are those with the highest surface temperatures and are blue in colour.

The dimmest objects in the sky are red in colour and lie in the lower right-hand end of the main sequence. Our sun lies at a point about in the middle of the main sequence. The stars lying on the main sequence with luminosities less than that of the sun are often given the collective name *dwarfs*.

Another important class of stars appearing on the H-R diagram is the large group above and to the right of the main sequence. These stars are fairly luminous, having an absolute bolometric magnitude near zero, but

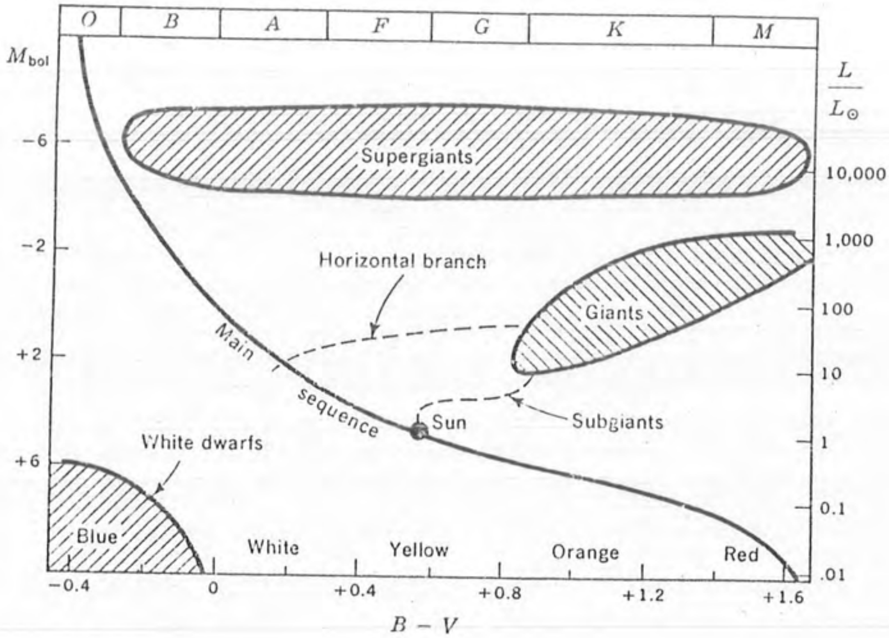

Figure 1.2. A schematic representation of the heavily populated areas in the H-R diagram. A high percentage of stars lie near the main sequence. The next most populous groups are the white dwarfs and the giants. (Taken from *Principles of Stellar Evolution and Nucleosynthesis* by Donald D. Clayton.)

they are very red in comparison with main sequence stars of the same luminosity. This class of stars is called collectively the *red giants*. The redness of these giants is balanced by their relatively large radii, leading to a significant luminosity.

A relatively small number of stars, called *subgiants*, are also shown in the H-R diagram. These are believed to be stars whose envelopes are expanding while their helium cores contract to a point where the helium begins to produce energy by nuclear reactions. Stars are also found on a horizontal branch to the left of (bluer than) the giant region. These stars are believed to be in various phases of helium burning.

There is also a class of very luminous stars ($L \approx 10^4\ L_\odot$) of all colours that spreads in a horizontal strip across the top of the H-R diagram. Collectively called *super giants*, these stars are probably in advanced stages of stellar evolution and are perhaps approaching the end of their energy-generating lifetime.

Far below the main sequence in the lower left-hand part of the H-R diagram lies another important class of stars, the *white dwarfs*. These stars are very much smaller than the sun in radius, although many of them have masses comparable to the sun. They are, therefore, highly dense objects with high surface temperatures, making them blue or white with low luminosity. We will discuss these objects in some detail in the next chapter. Numerically, the main sequence contains more stars than all the other groups put together, but the white dwarfs are the next most numerous class, perhaps 10 percent or so of all stars.

1.6 STELLAR INTERIORS

In order to study the interior structure of stars one attempts to apply the known laws of physics to stellar interior conditions in order to come up with a theoretical model of a whole star which is compatible with observations.

Spherical symmetry and hydrostatic equilibrium are fairly good approximations and apply to most of the stars. Spherical symmetry means that physical conditions are functions of only one variable, namely the distance r to the centre of the star. The condition of hydrostatic equilibrium requires that the sum of the outward force on an infinitesimal element, due to pressure, and the inward force on the element, due to gravity, be zero.

If the element of mass dm has the cross sectional area dA perpendicular to r, then this condition is expressed by the relation

$$- (dP)(dA) - gdm = 0 , \tag{1.4}$$

where P denotes the total pressure arising from all sources (pressure due to radiation as well as the gas pressure) and g is the magnitude of the gravitational acceleration at r:

$$g = \frac{GM(r)}{r^2} , \tag{1.5}$$

where $M(r)$ is the mass enclosed within a sphere of radius r and G is the constant of gravitation. Since

$$dm = \rho(r)(dr)(dA) , \tag{1.6}$$

where dr is the radial thickness of the element and ρ is its density, we may write the equation of hydrostatic equilibrium for spherical symmetry in the form

$$\frac{dP}{dr} = - \frac{GM(r)}{r^2} \rho(r) \tag{1.7}$$

The minus sign means that pressure increases as the radial distance decreases.

The mass distribution follows directly from the assumption of spherical symmetry. It is clear that we can write, for the mass of a spherical shell of matter of density ρ, radius r, and thickness dr,

$$dM(r) = 4\pi r^2 \rho(r) dr. \tag{1.8}$$

We now combine Eqs.(1.7) and (1.8) to obtain

$$- dP = \frac{G}{4\pi} \frac{M(r)}{r^2} dM(r) , \tag{1.9}$$

which is another form of the equation of hydrostatic equilibrium.

An integral expression for the *central pressure* P_c can be obtained immediately by integrating Eq. (1.9) over the whole stellar mass. In so doing we assume that $P = 0$ at $r = R$, where R is the radius of the star. The desired expression is then

$$P_c = \frac{G}{4\pi} \int_0^M \frac{M(r) dM(r)}{r^4} , \tag{1.10}$$

where M is the total mass of the star. This formula expresses the fact that for a star in hydrostatic equilibrium the central pressure must be great enough to support the weight of all the overlying layers. This weight of all the overlying layers, given by the right side of Eq. (1.10), may be interpreted as the central value of the "gravitational pressure".

If the density is taken as a constant equal to

$\bar{\rho}$, then Eq.(1.8) can be immediately integrated to give

$$M(r) = \frac{4}{3}\pi r^3 \bar{\rho}, \tag{1.11}$$

which is obvious for constant density. Substitute this expression into Eq.(1.7) and integrate over r to R, again using the fact that the pressure goes to zero at the surface:

$$P(r) = \frac{4}{3}\pi G\bar{\rho}^2 \frac{R^2 - r^2}{2}$$

$$= \frac{G\bar{\rho}M}{2R}\left[1 - \frac{r^2}{R^2}\right]. \tag{1.12}$$

In particular, the pressure at the centre of the star is

$$P_c = P(0) = \frac{G\bar{\rho}M}{2R}. \tag{1.13}$$

Taking the sun as a typical example, the mass of the sun is 2.0×10^{33} gm, and its radius is 7.0×10^{10} cm. This corresponds to an average density of 1.4 gm cm^{-3}. In the photosphere (the inner atmosphere of a star) the density is 10^{-7} gm cm^{-3} or less, and toward the centre it must get well above the average value. If it is assumed that the density is constant throughout the sun, then putting the numerical values for the sun in

Eq.(1.13) one finds that $P_c = 1.3 \times 10^{15}$ dyne cm^{-2} which gives a rough idea of the pressure to be expected in the solar interior. This pressure is about 10^9 atmospheres, and matter cannot retain the cohesion of a solid or a liquid under this tremendous pressure. The assumption that stars are gaseous throughout is then justified.

Two other useful quantities are the *mean temperature*, $\bar{T}$, and the *mean pressure*, $\bar{P}$, defined by

$$\bar{T} = \frac{1}{M} \int_0^M T dM(r) \tag{1.14}$$

and

$$\bar{P} = \frac{1}{M} \int_0^M P dM(r) \ . \tag{1.15}$$

Integrating Eq.(1.15) by parts, noting that the integrated term vanishes since $P(r) = 0$ and $M(0)=0$, and using Eq.(1.8), we obtain

$$\bar{P} = \frac{G}{4\pi M} \int_0^M \frac{M^2(r) dM(r)}{r^4} \ . \tag{1.16}$$

1.7 EQUATION OF STATE

The equation of state of an ideal gas is found to hold closely in most stars. This equation can be put into the form

$$P = \frac{k}{m} \rho T \ , \tag{1.17}$$

where T is the temperature, k is the Boltzmann constant and m is the mean molecular weight.

Typical temperatures to be expected in stellar interiors can be found from this equation. Since this is only to be a crude calculation, one is justified in assuming that the material is pure hydrogen. Anticipating rather high temperatures, one can also assume that the hydrogen is completely ionized, and thus that the matter consists of equal numbers of protons and free electrons. This means that the average mass per free particle m is essentially one-half of the proton mass, or about 0.8×10^{-24} gm. When the pressure and mean density found in the last section are put into Eq.(1.17), the temperature turns out to be 5.6×10^{6} K. Thus we find, for a typical temperature in the stellar interior, 10 million degrees Kelvin.

1.8 ENERGY LOSS

Energy loss at the surface, as measured by the luminosity of the star, is compensated for by the energy released from nuclear processes throughout the stellar interior. This condition may be expressed by the equation

$$L(r) = \int_0^R \varepsilon(r)\rho(r)4\pi r^2 dr \quad , \tag{1.18}$$

where ε is the energy released from nuclear processes per gram per second. This nuclear energy production will depend on temperature, density, and composition. In differential form Eq.(1.18) can be written as

$$dL(r)/dr = 4\pi r^2 \varepsilon(r)\rho(r) \quad , \tag{1.19}$$

which gives the energy balance for a spherical shell of radius r. The left-hand side of this equation represents the net loss to the shell caused by the excess of the flux leaving the shell through the outer surface over the flux entering the shell through the inner surface. The right-hand side represents the energy produced within the shell by nuclear processes. Eq.(1.19) represents the third of the basic equilibrium conditions which must hold throughout the stellar interior.

1.9 STELLAR EVOLUTION

The theoretical approach to stellar evolution is based on H-R diagrams. These diagrams suggest that stars begin their lives on the main sequence, but they must evolve onto the main sequence from some previous state. This previous state must be the tenuous gas and dust that exist between the stars called the interstellar medium. The interstellar medium is not exactly uniform, there being large irregularities in the density. Occasionally the density at a given region will become great enough for gravitational attraction of the material in this region to draw together and condense out of the general medium.

When an object of stellar mass has first condensed out of the interstellar medium, it is very large, tenuous, and cool. The contraction results in a loss of gravitational potential energy which, at first, causes the collapse to proceed more rapidly. The internal pressure eventually builds up to a point at which the collapse slows down, and the star comes almost into hydrostatic equilibrium. If the object has enough mass, the internal density and temperature will eventually become great enough for nuclear reactions to start taking place. When these reactions take place fast enough to supply the energy being radiated away, gravitational contraction stops and the star has arrived on the main sequence.

A star begins its career on the main sequence with a homogeneous composition. As hydrogen is being converted into helium in the central parts, the features of the star change, very slowly at first, more rapidly as the hydrogen becomes more nearly depleted at the centre. Then the hydrogen content in the centre becomes too low for nuclear reactions to supply enough energy to support the star against gravity. Gravitational contraction then becomes an important energy source as the inner parts of the star contract, while the outer parts expand. The star rapidly becomes brighter and cooler and moves upward and to the right in the H-R diagram, toward the red-giant region.

The contraction of the core of the star causes the central region to become hotter and denser, and hydrogen burning in shells further out from the centre can take place. Eventually conditions in the centre will become extreme enough for the nuclear burning of helium to form carbon. The star will then settle down to a second period of nuclear burning. Eventually, a point will be reached where even the helium in the deep interior is also exhausted. At the time the star will undergo further gravitational contraction, and the by-products of helium burning begin to be heated toward the temperature at which they will undergo nuclear reactions. After its time in the giant region the luminosity of the star must eventually begin to decrease unless the star ends its lifetime catastrophically. If it burns out slowly, its radius will shrink, and the surface temperature of the star will begin to increase again. Such a star will end eventually in its probable fate as a white dwarf. In the trip from the red-giant region to the white-dwarf region of the H-R diagram, each star that is to remain visible must reduce its mass below a certain value known as the *Chandrasekhar limit*. Failing to achieve a sufficiently small mass, the star will encounter a spectacular thermonuclear detonation called a *supernova explosion*. During this cataclysm, the star is completely torn apart and its burned-out core may implode to form a white dwarf, neutron star or black hole. These incredibly dense objects are the subject of discussion for the next chapter.

2

COMPACT OBJECTS

When all thermonuclear sources of energy are exhausted, a star will gradually cool down. A series of investigations has been made, since the 1930s, on the question of the end result of a "cold" star. The basic conclusions involve two main aspects. The first is that a star in the cooling process will collapse gravitationally, and form a superdense object called a compact star; second, these compact stars can be divided generally into three types: white dwarfs, neutron stars and black holes. Their study is important in relation to compact supernova remnants. The properties of neutron stars are important for theories of pulsars and compact X-ray sources. Neutron stars also represent the most compact objects known that can resist gravitational collapse to a black hole. Also, these are the kind of objects in which relativistic effects should be significant.

2.1 DEGENERACY

The equation of state of a gas discussed in section 1.7 is not for the complicated case of degeneracy. Degeneracy occurs at high densities. It is not necessarily caused, however, by the gas density approaching nuclear densities. Nuclear densities are of the order of 10^{12} gm cm^{-3} [2], which is more than a factor of a *thousand* higher than the highest densities which we encounter in (ordinary) stars. Rather, degeneracy is a direct consequence of the exclusion principle.

At low densities, for a given temperature, the number of particles per unit volume is quite small compared to the number of low energy states available to them; as a result the gas is not affected appreciably. But at higher densities for the same temperature, the lower energy levels become nearly filled up. The exclusion principle states that at most two electrons —— differing from each other in their spin —— may be contained in each level. As more particles are squeezed into the same volume, they must take on energies that are much higher than average; so a degenerate gas has much greater energy per particle. When the density is so great that all levels below a certain high energy level are completely filled, then the properties of the gas become dependent only on the density and the positions of the energy levels. The material is completely degenerate, and its characteristics no longer depend upon the temperature. By raising the temperature enough, however, the degeneracy can be removed. Because of the large energies of degenerate gases, the velocities often become quite large, and special relativistic effects come in.

2.2 WHITE DWARFS

A star after exhausting the accessible nuclear fuel will commence a profound contraction. For the result of this contraction two alternatives appear plausible. the contraction may lead to very high temperatures, so that completely new physical phenomena may completely dominate the final evolution phases. Or the contraction may lead to very high densities so that degeneracy occurs not only in the core but virtually throughout the star. This situation permits the star to settle into a final state little affected by the continual loss of residual energy from the surface.

This second evolutionary alternative then suggests that the final state of a star may be represented by the white dwarfs, which from their observed masses and radii, are known to have densities as large as 10^6 gm cm^{-3} [3]. This high density confirms that the electron gas in the main part of white dwarfs is very highly degenerate and the star is supported by the exclusion principle repulsion between electrons in its matter.

White dwarfs get their name from the fact that many of them are rather hot, thus having white colours, yet they fall far below the main sequence. This means that they must have very small radii.

It was shown by S.Chandrasekhar that a star cannot become completely degenerate unless its mass is less than a certain limit. This limit depends on the composition of the star, but it is about 1.4 solar masses. The white dwarfs have masses well below the Chandrasekhar limit. Although white dwarfs are very faint and cannot be observed at great distances, the number of known white dwarfs is very large. This supports the idea that many, if not all, stars go through the white-dwarf stage.

The equation of state of the degenerate electron gas can easily be calculated. Let there be n electrons/cm^3 in a volume V, and so altogether nV

electrons. In momentum space (p_x, p_y, p_z) these electrons uniformly fill a sphere whose radius is the maximum momentum p_0 (or the threshold energy, the so-called Fermi energy, $E_0 = p_0^2/2m$). We therefore have a volume $(4\pi/3)p_0^3 V$ in phase space and with two electrons per phase cell of size h^3 (due to the Pauli principle) we obtain the relation

$$nV = \frac{2}{h^3} V \frac{4\pi}{3} p_0^3 \qquad (2.1)$$

or

$$p = \sqrt{2mE_0} = h \left(\frac{3n}{8\pi} \right)^{1/3}. \qquad (2.2)$$

Now the pressure, just as in an ideal gas, is given by the familiar formula

$$P = (2/3)\ n\bar{E}\ , \qquad (2.3)$$

where $\bar{E}$ denotes the mean energy per electron. We can find the relation between $\bar{E}$ and E_0. It is in fact (using the classical expression for kinetic energy, $E=p^2/2m$)

$$\bar{E} = \int_0^{p_0} E 4\pi p^2 dp \Bigg/ \int_0^{p} 4\pi p^2 dp$$

$$= \frac{3}{5}\frac{p_0^2}{2m} = \frac{3}{5} E_0 , \qquad (2.4)$$

and so we obtain the equation of state of a completely degenerate electron gas:

$$P = \frac{2}{5} nE_0 = \frac{8\pi}{15} \frac{h^2}{m} \left(\frac{3n}{8\pi}\right)^{5/3} . \qquad (2.5)$$

Here there is no further mention at all of temperature; that is precisely the characteristic property of degeneracy.

The relation between n and the density (in gm cm^{-3}) is most easily expressed in terms of the mass μ_E (in atomic mass units) of one electron. Then:

$$n = \rho / m_H \mu_E , \qquad (2.6)$$

where μ_E=1 for hydrogen, 2 for helium, etc.

An estimate, $\rho \approx 10^6$ gm cm^{-3}, for the density in a white dwarf may illustrate these relations: from Eq.(2.6) we then have $n \approx 10^{30}$ electrons/$cm^3$and from Eq.(2.5) a pressure of the degenerate gas of $P \approx 10^{17}$ atm., a million times higher than, for example, in the centre of the sun. For an ideal gas to have the same pressure, it would need to have a temperature of ~ 2×10^9K. We can use the equation of state $P \propto \rho^{5/3}$ together with our earlier estimate of the pressure in the interior of a star of mass M and radius R, that is (see section 1.6) $P \propto \rho GM/R$, and the trivial relation $\rho \propto M^3/R$, to obtain approximately a mass-radius relation for white dwarf stars, viz.:

$$R \propto M^{-1/3} \quad , \tag{2.7}$$

that is, the radius decreases with increasing mass.

Using the above relation we can also write down the luminosity $L = 4\pi R^2 \sigma T_e^4$. According to this expression for luminosity, white dwarf stars of mass M should have

$$L \propto M^{-2/3} T_e^4 \tag{2.8}$$

which gives the mass of white dwarfs as $0.6M_\odot$. However by using a special relativistic correction in our approximation scheme we get a mass greater than this but less than $1.4M_\odot$. Putting in the density estimate we get the white dwarf radius ~ 10^4 km.

2.3 NEUTRON STARS

In 1932 Landau pointed out [4] that there was another possible final state for a star, also with a limiting mass of about one or two times the mass of the sun but smaller in size than a white dwarf. These stars would be supported by the exclusion principle repulsion between neutrons and protons, rather than between electrons. They were therefore called neutron stars. Baade and Zwicky [5] also independently advanced the concept of neutron stars later, in 1934. These stars would have radii of only ten miles or so and a density of about 10^{14} gm cm^{-3}. To appreciate what this high density signifies, a cupful of material from a neutron star would weigh as much as our earth!

In neutron stars the gravitational force is balanced by the pressure of degenerate neutrons. We know from the discussion of white dwarfs that the pressure of degenerate electrons is dominant when the density of matter is about 10^6 gm cm^{-3} [4]. If the density of matter increases further, the Fermi momentum of electrons also increases producing the following reaction in which a relativistic electron transmutes a nucleus of charge Z and atomic number A by inverse beta decay:

$$P + e^- \longrightarrow n + \nu_e \ ;$$

$$(Z, A) + e^- \longrightarrow (Z - 1, A) + \nu_e \ ;$$

the consequence of which is the neutronisation of the matter. After that, the pressure of degenerate neutrons becomes dominant and the star consists mostly of a degenerate neutron gas.

The density of a real neutron star varies from its centre to its surface. A possible structure is shown graphically in Figure 2.1.

A neutron star has a solid outer shell, with a depth of about 1 km, composed of a lattice structure of nuclei and degenerate free electrons. The density in the outer shell is about 10^6gm cm^{-3}, where the major type of nucleus is ^{56}Fe. As one goes deeper starting from the surface, one would find that the density of matter and the Fermi momentum of electrons would gradually increase, and after entering the neutronisation region the nuclei would have more and more neutrons, becoming neutron-rich nuclei. When the mass density is about 4.3×10^{11}gm cm^{-3}, free neutrons begin to form, and the matter in this domain is composed of nuclei which form the lattice, free electrons and free neutrons. When the density rises to about ~ 10^{14}gm cm^{-3}, the nuclei would disintegrate completely and a kind of fluid would be formed in which there would be few protons, electrons and muons. This is the neutron fluid region of neutron stars.

In the neutron fluid region the neutrons form

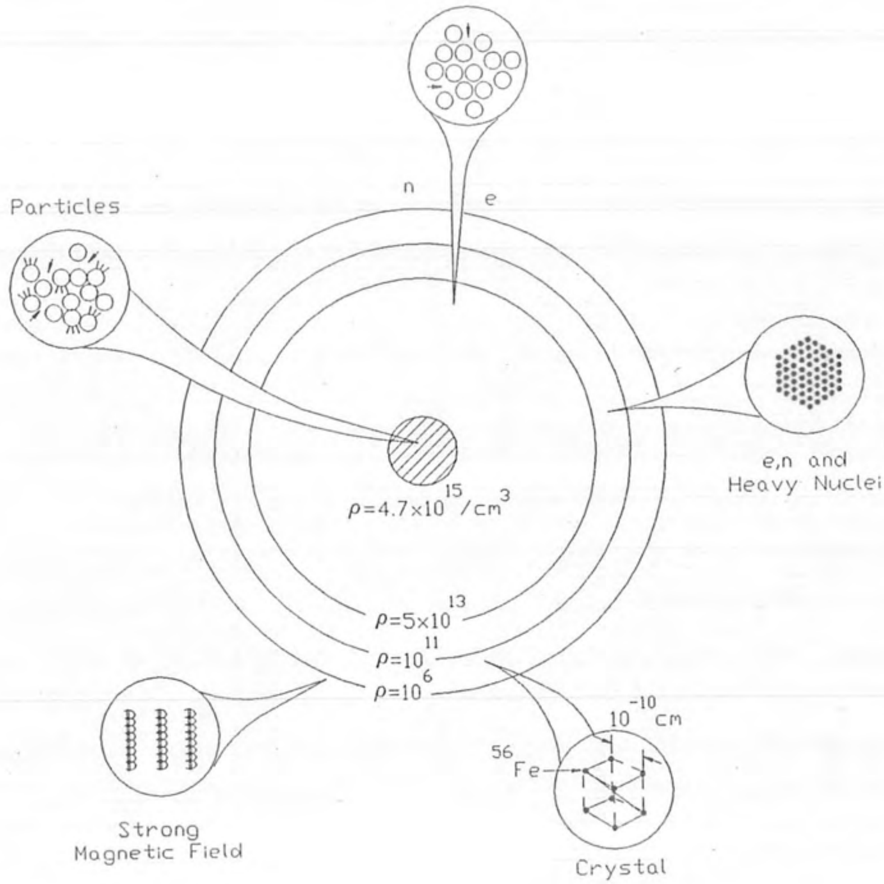

Figure 2.1. Possible internal structure of a neutron star. (Taken from *Basic Concepts in Relativistic Astrophysics* by L.Z. Fang and R. Ruffini.)

a superfluid, the protons are in a super conducting state, and the electrons constitute a Fermi-degenerate gas. This region continues to a density of the order of 10^{15} gm cm^{-3}.

For the case when the mass density exceeds 10^{15} gm cm^{-3}, there are different conclusions about the composition and the equation of state.

The lower mass limit of the neutron star is in the neighbourhood of 0.18 $M_{\odot}$. There is an upper mass limit characteristic to the neutron star. This is the mass limit set by general relativistic conditions. Because of high density, the general relativistic parameter GM/Rc^2 is close to 0.1, and general relativistic effects must be taken into account. The most important consequence for stellar structure is [6]:

$$\frac{dP}{dr} = - \frac{G(\rho + P/c^2)(M(r) + 4\pi r^3 P/c^2)}{r^2(1 - 2GM(r)/rc^2)} \quad . \qquad (2.9)$$

Compare this equation with Eq.(1.7) for the nonrelativistic case. We see that the effect of general relativity is to require a greater pressure gradient to achieve equilibrium. The upper mass limit for neutron star is 3.2 $M_{\odot}$ ——— the Fang-Ruffini limit.

2.4 BLACK HOLES

When the core of the collapsing star is too massive or imploding with too much kinetic energy, or both, the nuclear forces will not stop the implosion. Gravitational forces become more and more overwhelming and the system zooms through the neutron star stage and complete collapse occurs. The resulting system has been variously termed "continuing collapse", a "frozen star" and a "black hole".

According to K.Schwarzschild the gravitational field of a mass M which gives the planetary motions, can be represented by using the metric [7]

$$ds = \frac{dr^2}{(1 - r_s/r)} + r^2(d\theta^2 + \sin^2\theta\, d\varphi^2) - (1 - r_s/r)c^2dt^2, \tag{2.10}$$

in which r, θ, φ denote the usual spatial polar coordinates and t is the time.

The constant of integration

$$r_s = 2GM/c^2 \tag{2.11}$$

is called the gravitational (or Schwarzschild) radius of the mass M. Now if the radius of our body of mass M is less than r_s, then within the sphere $r \leq r_s$ the coefficient of the space-like element dr^2 and the time-like element $-c^2dt^2$ in Eq.(2.10) reverse their signs. This has the effect that neither matter nor even light quanta (and so also no kind of signal) can succeed in escaping from the region $r < r_s$, the so-called black hole, to the outside ($r > r_s$). A black hole is detectable by means of its gravitational field.

As mentioned earlier $M = 3.2M_{\odot}$ is the critical mass of a neutron star. It follows that there will be no other type of compact stars with masses greater than the critical value. Any cold star more massive than the critical value will collapse infinitely to form a black hole.

The evolutionary possibilities of a star can be reviewed by the summary given in Figure 2.2.

2.5 EXPLOSIVE STARS

The ancient astronomers had already noted that sometimes new stars become visible in the sky and after some time disappear again. In the Middle Ages the astronomers called these stars *novae*, which is the Latin word for new stars. In China such stars were said to be "guest" stars, because they usually appeared with an intensity visible to the naked eye for only a short while, to disappear like a visitor pressed for time. Their

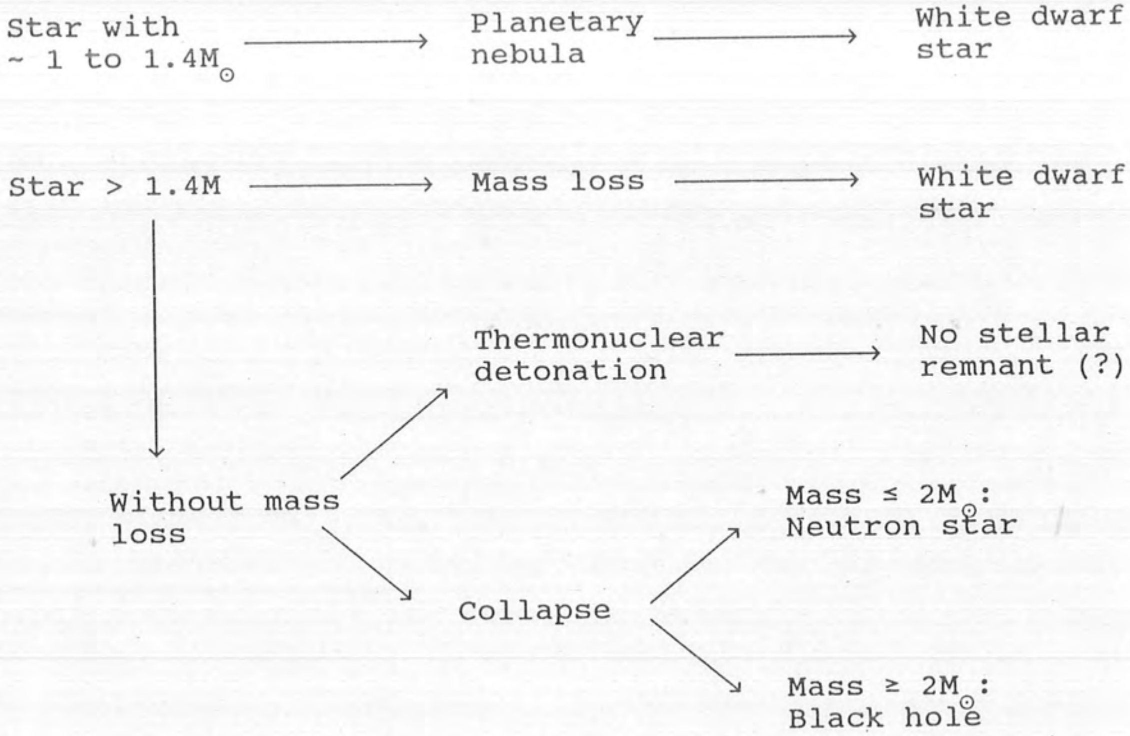

Figure 2.2. Evolutionary possibilities of a star. (Taken from *The New Cosmos* by A.Unsöld.)

lifetimes, between appearance and disappearance, differ from only several days for some to several months for others.

It was very rare to observe a nova with a life time exceeding half a year. After investigating the historical records of two thousand years, only eight novae with lifetimes greater than six months are found with an average of one appearing every three centuries [4]. They are called *supernovae*. Three of these supernovae were observed in historic times: Tycho de Brahe's supernova, which became very bright in the year 1604, and a supernova which was observed by Chinese astronomers in the year 1054. At the location of the Chinese supernova we now see the Crab nebula in the constellation of Taurus. The nebula got its name from its appearance which reminds one of a crab. The Crab nebula still expands with an average velocity of about 1400 km sec^{-1}, showing that a truly gigantic explosion must have occurred about 940 years ago.

Both novae and supernovae are objects which suddenly increase their light output by many orders of magnitude. They are usually not visible before the outburst so they appear as new stars. Since they had not previously been observed with the help of modern instruments we did not really know directly what types of objects the progenitors were. Then a very unusual supernova was observed in the Large Magellamic Cloud in February 1987 (SN1987a), for which the progenitor has been observed before and was classified as a B3Ib supergiant [8].

Before the explosion, the evolution of a supernova is just the evolution of the pre-supernova star. A general trend in advanced stages of stellar evolution is the formation of a red-giant structure. These may be a fairly extensive circumstellar shell. Figure 2.3 is a sketch illustrating some qualitative features of a pre-supernova star.

The luminosity of the supernova explosion is $\sim 10^{53}$erg sec^{-1} while the luminosity of the sun is 3.83×10^{33}erg sec^{-1}. The sun in its total life ($\sim 10^{10}$years) emits energy $\sim 10^{51}$ergs, which is less than the luminosity of the explosion. The supernova in its outburst, in fact, gives off more energy than does the whole observable universe ($\sim 10^{52}$erg sec^{-1})!

Supernovae are not very frequent events, so we cannot observe them in only one galaxy, but have to combine observations from many galaxies. Novae are less bright and more frequent. They can best be observed in

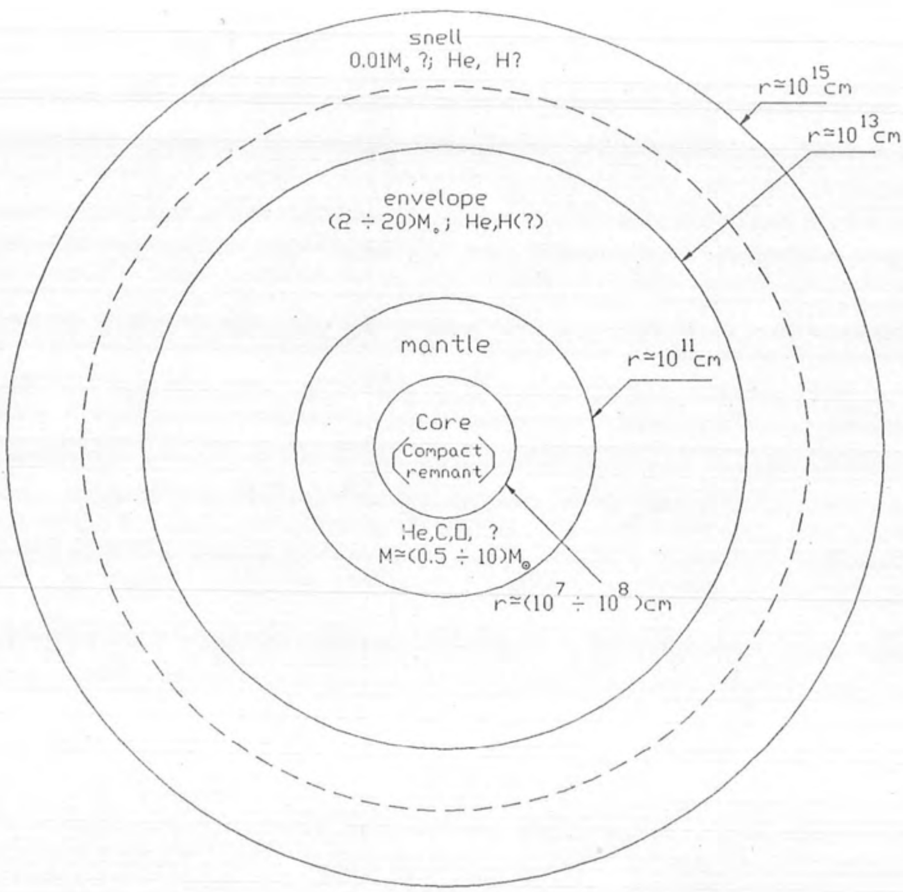

Figure 2.3. Schematic diagram of a supernova. (Taken from *Physics and Astrophysics of Neutron Stars and Black Holes*, eds. R.Giacconi and R.Ruffini.)

nearby galaxies and in our own galaxy. The one supernova observed in the Andromeda nebula, also called M31, had a maximum apparent magnitude m_w between 7 and 8, while the supernova 1987a observed in the Large Magellamic Cloud reached a maximum apparent brightness of 2.9 magnitudes [8]. It clearly appeared much brighter than any other extragalactic supernova observed so far.

With a distance of 700 kpc = 7×10^5pc (1 pc = 3.261633 light years = 3.085678×10^{18} cm) the absolute magnitude at maximum light for the Andromeda supernova was (neglecting interstellar absorption)

$$\begin{aligned} M_w &= m_w - 5 \times 4.85 \\ &= m_w - 24.3 \\ &= 7.3 - 24.3 = -17. \end{aligned} \tag{2.12}$$

For the 1987 supernova we find, using a distance modulus of $m_w - M_w = 18.3$, an absolute magnitude at maximum visual light of

$$M_w = 2.9 - 18.3 = -15.4. \tag{2.13}$$

If we compare this value with the absolute magnitude $M_w = -8$ for the brightest 'normal' star in the galaxy, or with the solar magnitude of $M_w = +4.8$, the supernova is 23 magnitudes brighter, or as bright as 10^9 suns, in the visual. Actually, the average M_w for supernovae appears to be $M_w \sim -1.8 \pm 1$ [8].

According to the records of the Chinese astronomers, the Taurus supernova reached a maximum apparent visual magnitude of about -5, which means it was visible during day time. For Tycho's supernova the maximum m_V was about -4 and for Kepler's about -3. The brightness of a supernova decreases exponentially with time. After one or two years it becomes invisible.

Altogether, several hundred supernovae have been observed. Unfortunately, none has occurred in our own Galaxy lately.

2.6 SUPERNOVA REMNANTS

A supernova explosion releases $E_{rel} = 10^{52}$ ergs or more energy as photons, neutrinos, and gravitational radiation. Since the binding energy of the presupernova core is typically $B_\omega \simeq -10^{48}$ ergs [3], the remant must have a binding energy $B_{rem} = B_\omega - E_{rel} \simeq -E_{rel}$. For remnant mass M_{rem} of order $M_\odot$, the imploded core must have average densities well in excess of those typical of the most massive white dwarfs. The only known objects that can be stable under such conditions are neutron stars.

Supernova progenitors ($M \geq 5M_\odot$) correspond roughly to spectral type B5 and earlier. If these stars rotate more or less rigidly, then their angular velocity $\Omega = v_e/R \approx 10^{-4}$ sec^{-1} [3]. Consider the collapse of a stellar core with this initial angular velocity. Its angular momentum is roughly $J \sim M_c R_c^2 \Omega$; assuming that J is constant during core collapse, the angular velocity of the remnant will be

$$\Omega_{rem} \simeq \Omega(R_c/R_{rem})^2 \sim 2 \times 10^4 \text{ sec}^{-1}, \qquad (2.14)$$

where we take $R_{rem} \sim 10^6$cm, as is typical for neutron stars. There is a limit to how rapidly a star can rotate, obtained by equating the gravitational and centripetal forces acting on an element of matter at the star's equator:

$$\Omega_{crit} \simeq (MG/R^3)^{1/2}. \qquad (2.15)$$

For a neutron star $\Omega_{crit} \approx 2 \times 10^4$sec^{-1}, which is the same as Ω_{rem} in Eq.(2.14). This suggests that compact supernova remnants may be formed in as rapid a state of rotation as possible. Rotation would then be dynamically important during collapse, since larger angular momenta generate centrifugal forces, which may balance gravitation near the equator. The subsequent evolution of the remnant mass might then be quite different from non-rotating configurations.

In several white dwarfs magnetic fields, having values as high as 10^7 gauss, have been detected. If we suppose that these fields are maintained during stellar evolution, and that they move with the matter as the star contracts, the magnetic flux will be conserved, and the average field during two different stages of evolution will satisfy [3]

$$B_2 \sim B_1 (R_1/R_2)^2 \qquad (2.16)$$

Assuming that this relationship applies to Am and Ap stellar types with $B_1 \simeq 10^3$ gauss and $R_1 \simeq R_\odot$ and further supposing that the magnetic field in the collapsing core of a presupernova satisfies this relation, then for $R_2 \simeq 10^{-4.7} R_\odot$ as is typical of neutron stars, $B_2 \simeq 10^{12}$ gauss. Fields of this magnitude will have a dramatic influence on the less-dense plasma surrounding the newly formed neutron star.

The arguments above indicate that compact supernova remnants may be rapidly rotating, magnetic neutron stars. The formation of a black hole is also possible, if the remnant mass is too great or as a result of mass accretion from matter originally ejected by the supernova.

A question arises here, do all supernova explosions leave a neutron star? In order to answer this, we have to know how a neutron star can be discovered. It has long been suggested that the Crab nebula is a remnant of the supernova outburst. The real confirmation came only when it was discovered that at the centre is what is called a *pulsar*. In the Vela remnant, another pulsar is found. The identification of pulsars with neutron stars provided the first observational evidence for these extremely compact objects. Previous observational searches for neutron stars had been confined to attempts to detect the thermal X-ray emission from neutron star surfaces ——— as John A.Wheeler has remarked [6], it was not realised that neutron stars would come equipped with a handle and a bell!

3

PULSARS

The discovery of radio pulsars in 1967 ranks among the most important and influential observations in modern astrophysics. These unique objects established the existence of neutron stars and their relation to supernovae. They were also a newly discovered source of cosmic rays, and offer a new method of estimating distances within our Galaxy. Observations of a binary system containing the pulsar PSR 1913+16 are the strongest current support for the existence of gravitational radiation as described by Einstein's theory of general relativity.

3.1 DISCOVERY OF PULSARS

One of the most remarkable discoveries in modern astronomy was the detection, in late 1967, of the clock like radio pulses emitted by objects that have come to be called pulsars. The discovery was made by Jocelyn Bell and Antony Hewish at Cambridge University. Their radio telescope array was designed to study the interplanetary scintillation of compact radio sources. The telescope is a rectangular array containing 2048 full-wave dipoles operating at 81.5 MHz and covering nearly five acres of land [6].

The group at Cambridge had great difficulty convincing themselves that the strange signals were being emitted by astronomical objects. The possibility of man-made signals transmitted from space probes or reflected from the moon or planets were ruled out because the absence of any parallax greater than about two arc minutes showed that the source lay far outside the solar system. Also the time duration of the emitted pulses was of the order of 20 ms and so, on the basis of light travel-time arguments, it was concluded that the source could not be larger than the earth. Bell and her supervisor even thought they might have made contact with an extraterrestrial civilization in the galaxy! Stephen

Hawking recalls: "Indeed, at the seminar at which they announced their discovery, I remember that they called the first four sources to be found LGM 1-4, LGM standing for "Little Green Men". In the end, however, they and every one else came to the less romantic conclusion that these objects, which were given the name *pulsars*, were in fact rotating neutron stars that were emitting pulses of radio waves because of a complicated interaction between their magnetic fields and surrounding matter" [9]. When three more similar pulsating sources were detected, it became clear that the sources had to be natural phenomena. The discovery of the first pulsar, PSR 1919+21, was announced by Hewish, Bell, Pilkington, Scott, and Collins on February 24, 1968, in the journal *Nature*.

The discovery had an enormous impact on the international astronomical community. Most of the larger radio telescopes in the world were directed toward PSR 1919+21, and a torrent of both observational and theoretical research papers began to flow into the journals. Most radio observations started looking for other pulsars and discovered many of them. Now about 500 of these sources are known.

3.2 BASIC PROPERTIES OF PULSARS

The signal observed from a pulsar is broad-band radio noise whose maximum intensity occurs at exactly periodic intervals of about 1 sec typically. The radio emission of PSR 0329+54, a typical pulsar, is shown in Figure 3.1, with an observed frequency of 410 MHz and a pulse period of 0.714 sec.

The conventional nomenclature for a radio pulsar is PSR *hhmm* ± *xx*, where the first four integers give its right ascension in hours and minutes, and *xx* denotes degrees of declination.

Pulsar periods have been observed to range from a few millisecond to 3.745 sec (for PSR 0525+21). Figure 3.2 shows the period distribution for 149 pulsars. The periods of all known pulsars show a gradual rate of increase, amounting typically to 10^{-13}—— 10^{-16} sec per sec (about 10^{-6}—— 10^{-9}sec per year). The extreme regularity and gradual rate of slowdown of the pulse are key features that theory must explain. The regularly increasing periods imply that pulsars are unlikely to be older than the *characteristic time*,

$$T = P\,\dot{P}^{-1}, \qquad (3.1)$$

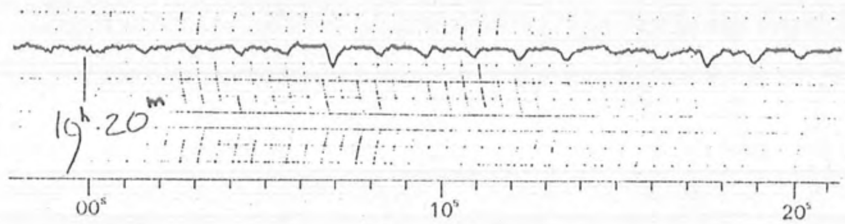

Figure 3.1. Chart record of individual pulses from one of the first pulsars discovered, PSR 0329 +54. The pulse period is 0.714 sec. The instrument time constant is 20 ms. (Taken from *Pulsars* by R.N.Manchester and J.H.Taylor.)

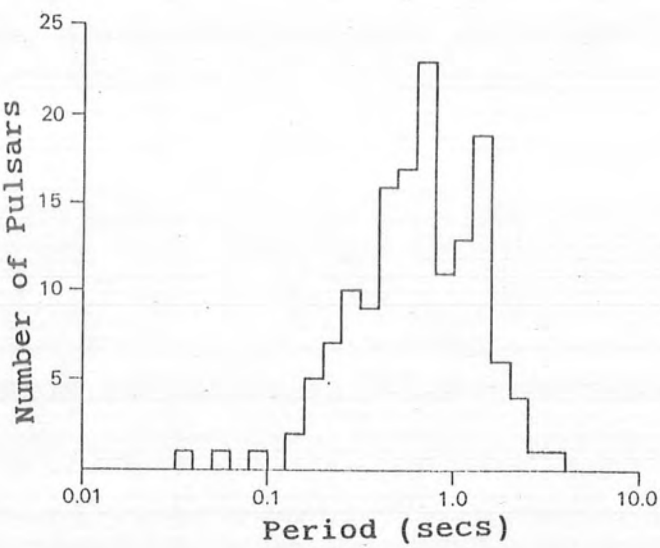

Figure 3.2. Pulsar period distribution for 149 pulsars. (Taken from *Pulsars* by R.N.Manchester and J.H.Taylor.)

typically about 10^7 years. For pulsars with shorter periods, rates of change are often larger and the characteristic time less; for the Crab pulsar, T = 2480 years. Table 3.1 gives the period P and its time rate of change; the dispersion measure; rotation measure, and distance for several pulsars.

Individual pulses are often found to consist of two or more *subpulses*, which frequently overlap and have characteristic widths of one or two percent of the period. A further precision reveals that within the subpulses some pulsars show *micro structure*, which has a characteristic width of about 0.1 percent of the period.

3.3 INTEGRATED PULSE PROFILES

The *integrated profile* is obtained by adding many individual pulses in phase. Despite the variable nature of subpulses in a given pulsar, the shape of the integrated profile is quite stable. Integrated profiles differ greatly from one pulsar to another. Integrated profiles for some pulsars, showing the wide variety of observed shapes, are given in Figure 3.3. About half of the known pulsars have profiles with a single peak or *component*. Two-component or "double" profiles are relatively common. Up to five components are seen in the

PSR	Period (sec)	dP/dt ($\times 10^{-15}$ sec per sec)	Dispersion measure (cm^{-3} pc)	Rotation measure (rad m^{-2})	d (kpc)	$\frac{1}{2}P/\dot{P}$ (10^6y)
0531 + 21 (Crab)	0.0331	422.69	56.7	−42.3	2.0	.0012
0833 − 45 (Vela)	0.0892	125.03	69.0	+33.6	0.5	.011
0525 − 21	3.7454	40.06	50.9	−39.6	1.9	1.5
1913 + 16 (binary pulsar)	0.0590	0.0088	167	——	6.2	-
1859 + 03	0.6554	7.50	402.9	−238	20	1.4
0329 + 54	0.7245	2.05	26.7	−63.7	2.6	5.5
1929 + 10	0.2265	1.16	3.17	− 8.6	0.1	3.1

Table 3.1. Observed parameters for seven pulsars. (Taken from *Astrophysics* by R.L. Bowers and T.Deeming.)

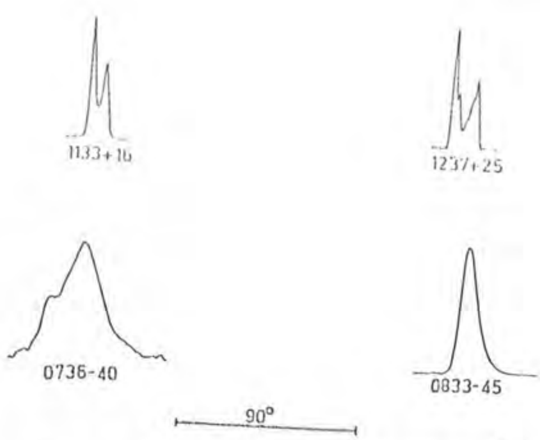

Figure 3.3. Integrated pulse profiles for several pulses plotted on the same longitude scale (a 90^0 bar is given in the bottom of the figure). (Taken from *Pulsars* by R.N.Manchester and J. H.Taylor.)

profiles of some pulsars. In some such cases the components are symmetrically disposed about the profile centre, so the profile still has a "double" appearance. For example, PSR 1237+25 (Fig. 3.3) has five distinct components, but is basically double in form.

In general, integrated profiles remain stable in shape and polarization on long time scales; this is of course the reason why they are an important feature of pulsar emission. Individual pulses vary greatly in shape, intensity, and longitude from one pulse to the next. Because of this, the stability of an integrated profile clearly depends on the number of pulses included in it. No long-term or secular change in the shape of integrated profiles or their intrinsic polarization has ever been detected. Helfand, Manchester, and Taylor [6] investigated the long-term stability of the profiles of four pulsars over an interval of about three years and found no case in which the variations exceeded those expected on the basis of the number of pulses included in the profiles.

3.4 PULSAR MODELS

Cosmic radio sources have been known to exist for about fifty years. The startling aspect of pulsars that theory first addressed was the clock like precision of their signal, i.e., periods on the order of tenths of a second that remained constant to within a few nano-seconds per year. Three distinct mechanisms were seen as possibilities for producing the periodic signals: radial pulsations, orbital motion and rotation. Radio emission is observed from interstellar plasma, but the extreme regularity of pulsars ruled this out. Sharp features in the radio pulses of duration $\Delta t < 10\ \mu$ sec are observed. For coherent radiation this implies an emitting region smaller than $c\Delta t$, or about 10 km in extent. White dwarf or neutron stars are the only objects compatible with these energy and size requirements.

Stellar pulsations (vibrations) are one mechanism capable of producing a regular train of signals. A star's pulsation period is approximately proportional to $\rho^{-1/2}$, where ρ is the mean stellar density. For typical white dwarfs, $\rho \sim 10^{6}$ gm cm^{-3} or less, which implies a period of 10 sec or more. Even for $\rho \sim 10^{8}$gm cm^{-3}, we find $P > 1$ sec, which is far too long for most pulsars. In fact, the discovery of the pulsar in the Crab nebula has ruled out this model, because the period of this pulsar is only 0.033 sec. For neutron stars $\rho \sim 3 \times 10^{14}$ gm cm^{-3}, and the period associated is of the order of

10^{-4} sec —— more than a factor of 10^2 too fast.

A binary system might also sustain a regular pulsed signal. By means of Kepler's third law , the period P, semi-major axis a, and stellar masses may be related. Periods of less than a second require [3]

$$a = 1.5 \times 10^8 \ (P \ \mu \ \text{sec})^{2/3} \left[(M_1+M_2)/M_\odot \right]^{1/2} \text{cm.} \qquad (3.2)$$

Only for a neutron star and a black hole, or for two black holes, would a exceed the radius of the stars. In either case, the binary system would be a strong emitter of gravitational radiation that would cause large energy loss and the period would shorten quickly. This is contrary to observational results where the period increases slowly.

As for the rotation mechanism, the period of rotation of a compact mass must be such that the equatorial angular acceleration does not exceed the gravitational acceleration at the surface. This requires that [3]

$$P_{rot} \gtrsim (3\pi/\rho G)^{1/2} = 1.2 \times 10^4 \ / \sqrt{\rho} \ \text{ sec.} \qquad (3.3)$$

For a white dwarf the period cannot be smaller than 1 sec. In order to ensure that the speed of a point in the equatorial plane of the star does not exceed the speed of light, the radius of the pulsar in the Crab nebula should be smaller than 1700 km. Only the radii of neutron stars can be smaller than this value. (As long as pulse-emission models require magnetic fields, rotating black holes, which cannot possess magnetic field, must be excluded.) Also, rotating neutron stars easily cover the entire observed range of periods. So of all the models considered, a rotating neutron star seems to be the most suitable candidate for a pulsar.

3.5 THE ROTATING NEUTRON STAR MODEL

The rapidly spinning neutron star, first considered by Pacini [10] and first proposed as a pulsar model by T.Gold [11], gained support as the simplest and most flexible method of obtaining periods in the observed range. Baade and Zwicky [5] had suggested, long before the discovery of pulsars, that neutron stars would be found in supernova explosions. The association of the two pulsars (the Crab and the Vela pulsars) having the shortest periods, known at the time, with known supernova remnants gave further support to this interpretation. The existence of the Crab pulsar also fulfilled predictions made by Wheeler [12] and Pacini [10] before the discovery of pulsars, namely, that the energy source in the Crab Nebula could be a rotating neutron star.

Gold accommodated all the observations in the "lighthouse beacon" model (Fig. 3.4) according to which every rotation of the ultra-dense star sweeps a lighthouse beam over us and the pulse period is equal to the rotation period of the star. The high magnetic field (~ 10^{12} gauss) and high rotation rate about the axis, generally out of alignment with the magnetic axis, would cause the plasma to emit dipole radiation in a particular direction. The rotation of the star would cause the radiation to move like a lighthouse beam which would be seen as pulses of electromagnetic radiation on Earth.

Consider the neutron star in the Crab nebula. To calculate the energy loss due to rotation, which we know by observation to be of the order of 10^{38} ergs, we use the equation relating the rotational energy of the star , E_{rot} , to the moment of inertia, I [13],

$$E_{rot} = \frac{1}{2} I\omega^2, \tag{3.4}$$

where ω is the angular speed (measured in radians per unit of time). Assuming that the moment of inertia does not change with time, we get

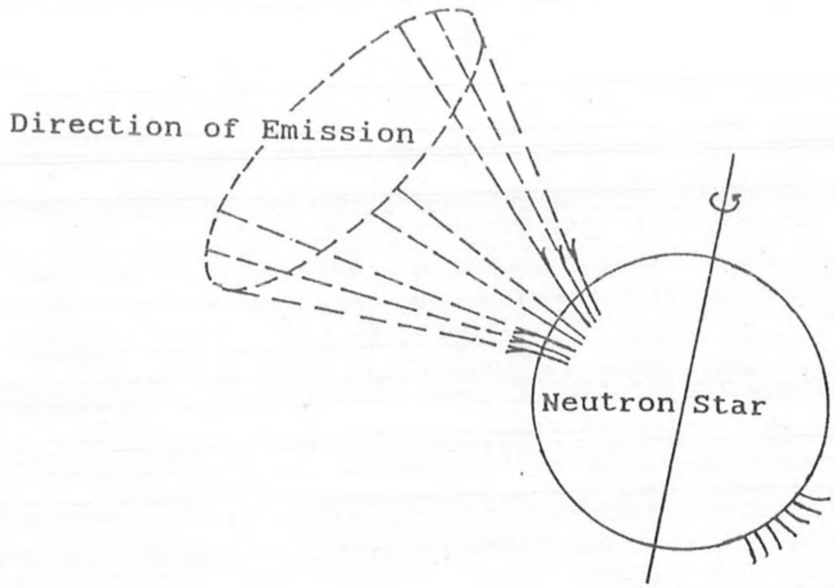

Figure 3.4. Artists conception of the lighthouse beacon model of a pulsar. (Taken from *The Physics of Pulsars*, ed. A.M.Lenchek.)

$$\left[\frac{dE}{dt} \right]_{rot} \approx I\omega \frac{d\omega}{dt} . \qquad (3.5)$$

Now, the rate of change of the period for the Crab pulsar is $\dot{P} \approx 13.5$ microsec per sec. This gives the rate of rotational energy emission being, roughly, 4.8×10^{38} erg sec^{-1} which is a very good fit with observation.

The radiation from pulsars was believed [13] to be purely dipole in nature. In this case the pulsar frequency, ω, and its derivative $\dot{\omega}$, are related by

$$\dot{\omega} = \alpha\omega^3, \qquad (3.6)$$

where α is a constant for a given pulsar and is related to its moment of inertia. Also the rate of slowing of the pulsar can provide an estimate for the age of the pulsar [14]

$$T = \int_0^T dt \approx \int_{\infty}^{\omega} d\omega/\dot{\omega} , \qquad (3.7)$$

where T is the present age and ω is the present pulsar frequency. Also it is assumed that the initial pulsar frequency is much greater than the present value. For the purely dipole radiation , the braking index,

$$n = \omega \, \ddot{\omega} \, / \dot{\omega}^2 , \qquad (3.8)$$

should be 3. But there are some problems. For the Crab pulsar n = 2.515 ± 0.005 (as of 1969, when the age was 915 years). Also $\omega_p \approx 3.9 \times 10^{-19}$ Hz $sec^{-1}$and $T \approx 2.9 \times 10^{10}$ secs. Eqs (3.6) and (3.7) taken together give $T \approx 3.9 \times 10^{10}$ secs (about 1240 years).

3.6 ANOTHER MODEL

The Gold model of the pulsar as a fast rotating neutron star with a high magnetic field is entirely satisfactory as far as it goes. This model explains the finer details of the observations as being due to the internal structure of the neutron star. But as has been pointed out earlier, there are some problems with this model.

The standard model gives a low value for the braking index. It was supposed that this discrepancy could be removed by considering the higher multipole moments. It has been pointed out [15], however, that higher pole moments cannot reduce the value of n but would, in fact, increase it. There is a standard explanation [6] that Eq.(3.6) should be replaced by

$$\dot{\omega} = \alpha\omega^n \quad , \tag{3.9}$$

so that we get the correct value of n. Also, if we put in an unknown initial pulsar frequency, ω_i, we can determine ω_i from Eq.(3.7) instead of predicting T. This gives

$$\omega_i/\omega_p = \left[1 + (n - 1)\ \dot{\omega}_p T/\omega_p \right]^{1/(1-n)} . \qquad (3.10)$$

For the Crab pulsar this ratio is about 1.715. This is an unsatisfactory explanation in that instead of predicting it only 'explains'. Also the standard model does not explain the high cooling rate.

According to the standard model pulsars cannot have an initial frequency greater than 100 Hz as they would break up due to centrifugal forces. This is just compatible with the 'millisecond pulsars' observed, with frequencies of 10^3 Hz . These pulsars have $\dot{\omega} \approx 0$ and are explained as neutron stars which are accreting matter at a rate just enough to maintain their frequency. Thus they 'spin up' due to accretion as much as they 'spin down' due to radiation. However, using a formalism similar to the pseudo-Newtonian (ΨN) formalism [16], Abramowicz has shown [17] that the 'relativistic centrifugal force' need not always be repulsive. In fact in the regime relevant for the pulsar it will be *attractive* and will hold the pulsar together instead of causing it to break up!

An alternative suggestion [18] was that the low value of n was due to ohmic radiation caused by plasma heating in the rotating magnetic field. In effect the pulsar acts like a dynamo generator with the plasma playing the role of a resistance. Here the energy generation mechanism is provided by the plasma. The radiation field could then be expressed in terms of a multipole expansion with an 'ohmic' term added. A natural assumption for the ohmic term gives

$$\dot{\omega} = a\omega + b\omega^3 + c\omega^5 + \dots \quad . \tag{3.11}$$

The coefficients in the expansion would be slowly varying functions of time (compared with the variation of ω). Over a short duration they could be regarded as constants. Taking a relatively high initial pulsar frequency these constants could be estimated by fitting with the age estimation and the observed value of n. The high initial pulsar frequency was predicted [19], using angular momentum considerations, to be about 2×10^3 Hz.

A major deference between the two suggestions is that the latter envisages all pulsars as essentially different evolutionary stages of more or less the same object while the former allowed for much greater variation between pulsars at birth.

Also, there was no explanation, in the

standard model, provided for the drift velocity ~ 10^2 km sec^{-1} of the pulsars relative to their parent supernova remnants (to be discussed in more detail in the next section). The high value of the initial pulsar frequency predicted by the alternative model opened up an intriguing relativistic explanation of pulsar drift [20,21]. What is required is a decisive test between the two views.

3.7 PULSAR DRIFT

As discussed earlier, pulsars are expected to be found at the centres of supernova remnants and supernova remnants to be found around pulsars. However, only two pulsars, the Crab pulsar (PSR 0531+22) and the Vela pulsar (PSR 0833-45) out of the ~ 500 known pulsars, and a collapsed object [22] SS433 have been found within supernova remnants: the Crab nebula, Vela X and W50 respectively. Pulsars are assumed to have a drift velocity ~ 10^2 km sec^{-1} relative to their respective supernova remnants [6,23]. The Vela pulsar is, indeed, visibly off the centre of the Vela nebula.

Using the pseudo-Newtonian (ΨN) formalism [16] in general relativity it was argued [20] that the gravitational force that is expected to lead to the collapse of the stars also has an angular component, in addition to a radial component, because of which the centre of action of this force is not the geometrical centre of the star. This force could be asymmetric. This asymmetry could lead to the 'drift' of pulsars. Observational details of the explosion of the supernova 1987a seem to favour this argument.

In another analysis [24] an electromagnetic mechanism for pulsar drift was suggested. It was argued that the strong magnetic field of the nascent pulsar would drive the plasma surrounding it: the positively charged particles will move along a helix in one direction while the negatively charged particles will move in a helix in the opposite direction. The net effect will be to add angular momentum along the axis of the rotating sources, which produces an asymmetric force to cause the pulsar drift. The paths of the particles were roughly approximated by helices during the short period of the collapse and explosion as they cannot be expected to be exactly cylindrical helices. There is a strong need for more detailed calculations to see whether the pulsar is shot out of the supernova remnant by a 'magnetic rail-gun' effect or a 'gravito-magnetic rail-gun'.

4

MOTION OF CHARGED PARTICLES IN THE GRAVITATIONAL AND MAGNETIC FIELD OF A PULSAR

As discussed earlier pulsars commonly have large spatial velocities, often greater than 100 km sec^{-1}. There is a possibility that pulsars are given such a high velocities at birth as a result of asymmetries in the supernova explosion. Pulsar drift can be caused as a result of the net force due to the motion of negatively and positively charged particles in the plasma surrounding the nascent pulsar. To have a deeper insight into the problem one should exactly know the behaviour of these charges. In this chapter we will construct the equation of motion, taking into account the strong gravitational (~ 10^8 times larger than the earth's field) as well as magnetic field (10^{12} G typically) of a neutron star (not including the relativistic effects, presently) and solve them numerically.

4.1 VELOCITY AND ACCELERATION IN SPHERICAL POLAR COORDINATES

Let r, θ, φ be the usual spherical polar coordinates of a point P. Let $\hat{r}$, $\hat{\theta}$, $\hat{\phi}$ denote the unit vectors in the directions of r, θ, φ increasing, respectively. These constitute a right-handed frame for which $\hat{r} \wedge \hat{\theta} = \hat{\phi}$, etc. This frame has angular velocity [25]

$$\mathbf{w} = \dot{\theta} \ \hat{\phi} + \dot{\varphi}(\cos\theta \ \hat{r} - \sin\theta \ \hat{\theta})$$

$$= \dot{\varphi} \cos\theta \ \hat{r} - \dot{\varphi} \sin\theta \ \hat{\theta} + \dot{\theta} \ \hat{\phi}. \qquad (4.1)$$

Hence the velocity of P is

$$\mathbf{v} = d\mathbf{r}/dt = \partial\mathbf{r}/\partial t + \mathbf{w} \wedge \mathbf{r}$$

$$= \dot{r} \ \hat{r} + (\dot{\varphi} \cos\theta \ \hat{r} - \dot{\varphi} \sin\theta \ \hat{\theta} + \dot{\theta} \ \hat{\phi}) \wedge \mathbf{r}$$

$$= \dot{r} \ \hat{r} + r\dot{\theta} \ \hat{\theta} + r \ \dot{\varphi} \sin\theta \ \hat{\phi} \ . \qquad (4.2)$$

If R, S, T denote the three components of acceleration, **a**, we see that

$$
\left.\begin{aligned}
R &= \ddot{r} - r\dot{\theta}^2 - r\dot{\varphi}^2 \sin^2\theta. \\
S &= r\ddot{\theta} + 2\dot{r}\dot{\theta} - r\dot{\varphi}^2 \sin\theta \cos\theta. \\
T &= r\ddot{\varphi} \sin\theta + 2\dot{r}\dot{\varphi} \sin\theta + 2r\dot{\varphi}\dot{\theta} \cos\theta.
\end{aligned}\right\} \qquad (4.3)
$$

4.2 THE LORENTZ FORCE

In 1820 the Danish physicist Oersted discovered that a magnet which is able to move freely, lines up perpendicular to a wire conductor which carries a current. Other scientists showed that current carrying wires exert forces on one another. Later experiments with cathode ray tubes showed that the electron path is deflected by a current carrying wire. From these experiments we conclude that an electric current is accompanied by a magnetic field, or a magnetic field is associated with an electric current.

If a charged particle is sent into a magnetic field, it is deflected. The direction of the force, acting on the particle, is perpendicular to the direction of the magnetic field. Another fact, which was found experimentally, is that the force is proportional to the velocity, **v**. The proper direction of the force **F** can be found from the direction of the velocity by the introduction of the magnetic field **B**, so that the direction of **F** is the direction of the vector product **v** Λ **B**. Other experiments show that the force depends also on the charge q of the particle. We, therefore, introduce the magnetic field vector **B** so that it satisfies the relation [26]

$$\mathbf{F} = q\mathbf{v} \wedge \mathbf{B} \tag{4.4}$$

This force is called the Lorentz force, after the Dutch scientist H. A. Lorentz (1853-1928), and is consistent with the requirements of Special Relativity [27].

4.3 DIPOLE FIELD IN SPHERICAL COORDINATES

We know that the curl of the magnetic induction is zero wherever the current density is zero. In such regions, therefore, the magnetic induction can be written as the gradient of a scalar potential:

$$\mathbf{B} = -\mu_0 \nabla\Phi. \tag{4.5}$$

However, the divergence of **B** is also zero, which means that

$$\nabla.\mathbf{B} = -\mu_0 \nabla^2\Phi = 0 \; . \tag{4.6}$$

Thus Φ, which is called the magnetic scalar potential, satisfies Laplace's equation.

Now for a *magnetic dipole moment* **d**, we can write [26]

$$\mathbf{B} = -\mu_0 \nabla \left(\frac{\mathbf{d.r}}{4\pi r^3} \right) . \tag{4.7}$$

It is clear that

$$\Phi = \mu_0 \frac{\mathbf{d.r}}{4\pi r^3} , \tag{4.8}$$

where μ_0 is the *permeability* of free space. We can write Eq.(4.8) as

$$\Phi = \mu_0 \frac{\mathbf{d.r}}{4\pi r^3} = \mu_0 \frac{d\cos\theta}{4\pi r^3} , \tag{4.9}$$

where θ is the angle between **d** and **r**.

Now writing **B** in spherical coordinates, the vertical component of the field is

$$B_s = -\frac{\partial \Phi}{\partial r} = \frac{2\mu_0 d}{4\pi} \frac{\cos\theta}{r^3} , \tag{4.10}$$

and the horizontal component is

$$B_\theta = -\frac{\partial \Phi}{r\partial \theta} = \frac{2\mu_0 d}{4\pi} \frac{\sin\theta}{r^3} . \tag{4.11}$$

Finally

$$B_\varphi = 0 . \tag{4.12}$$

Thus the magnetic field has no azimuthal component.

4.4 EQUATION OF MOTION

Now for a charged particle of mass m and charge q, the equation of motion in the gravitational and magnetic field of a neutron star (using the Lorentz force law) can be written as

$$m\mathbf{a} = -m\mathbf{g} + q(\mathbf{v} \wedge \mathbf{B}), \tag{4.13}$$

where $g = MG/r^2$, M being the mass of the neutron star. We will be using the Gaussian system of units in which $\mathbf{B}$ in all the previous equations is replaced by $\mathbf{B}/c$ and $\mu_0 = 4\pi/c^2$ [26].

By the nature of the system it will be suitable to use spherical polar coordinates. Writing $\mathbf{a}$, $\mathbf{r}$ and $\mathbf{B}$ in Eq.(4.13) in spherical coordinates, given in Eqs.(4.2), (4.3), (4.10) —— (4.12) the three equations of motion read

$$m(\ddot{r} - r\dot{\theta}^2 - r\dot{\varphi}^2\sin^2\theta) = -mg - \frac{qd}{c^2}\,\frac{\sin\psi\,\sin\theta}{r^2}\,\dot{\varphi}, \tag{4.14}$$

$$m(r\ddot{\theta} + 2\dot{r}\dot{\theta} - r\dot{\varphi}^2\sin\theta\,\cos\theta) = \frac{2qd}{c^2}\,\frac{\cos\psi\,\sin\theta}{r^2}\,\dot{\varphi}, \tag{4.15}$$

$$m(r\ddot{\varphi}\,\sin\theta + 2\dot{r}\dot{\varphi}\sin\theta + 2r\dot{\varphi}\dot{\theta}\cos\theta) = \frac{qd}{c^2}\left(\frac{\dot{r}\sin\psi}{r^3} - \frac{2\dot{\theta}\cos\psi}{r^2}\right), \tag{4.16}$$

where dot ($\dot{}$) denotes differentiation with respect to time, and ψ here is the angle between **d** and **r**. Equivalently we can write these equations as:

$$\ddot{r} = - \frac{MG}{r^2} + \left(\frac{qd}{mc^2} \right) \frac{\sin\psi \sin\theta}{r^2} \dot{\varphi} + r\dot{\varphi}^2 \sin^2\theta + r\dot{\theta}^2, \tag{4.17}$$

$$\ddot{\theta} = - \left(\frac{qd}{mc^2} \right) \frac{2\cos\psi \sin\theta}{r^3} \dot{\varphi} + \dot{\varphi}^2 \sin\theta \cos\theta - \frac{2\dot{r}\dot{\theta}}{r}, \tag{4.18}$$

and

$$\ddot{\varphi} = \left(\frac{qd}{mc^2} \right) \left[\frac{\sin\psi\, \dot{r}}{r^4 \sin\theta} - \frac{2\cos\psi\, \dot{\theta}}{r^3 \sin\theta} \right] - \frac{2\cos\theta\, \dot{\theta}\, \dot{\varphi}}{\sin\theta} - \frac{2\dot{r}\dot{\varphi}}{r}. \tag{4.19}$$

This form is more convenient for numerical solution (see appendix). We take a typical pulsar with $M = M_{\odot}$ and $d = 2.5 \times 10^{30}$ gauss cm^3. When we solve these equations for a proton, at a distance of 8000 km from the centre of the neutron star at $\theta = \pi/4$, $\varphi = 0$ for $\psi = \pi/4$ and $\dot{r} = \dot{\theta} = \dot{\varphi} = 0$ at $t = 0$, the motion is as shown in Figure 4.1. The figure shows that the particle is first pulled towards the neutron star until it comes very close, where it gets pushed away to a distance of about 8000 km. This is because the gravitational force pulls the particle towards it and when it comes very close the strong magnetic field pushes it away. In this way the particle is put into a highly elliptical orbit. These results show that the particle always remains in the 'upper' hemisphere of the space around the star.

Similar orbits for a proton when it is 'introduced' at a distance of 800 km are shown in Figure 4.2. However, if the proton is initially very close, say 60 km it shoots out after one or two oscillations (Fig. 4.3).

Electrons are also put into elliptical orbits as shown in Figure 4.4 and 4.5. At somewhat smaller distance, 400 or 100 km, electrons initially come in and then shoot out (Fig. 4.6 and 4.7).

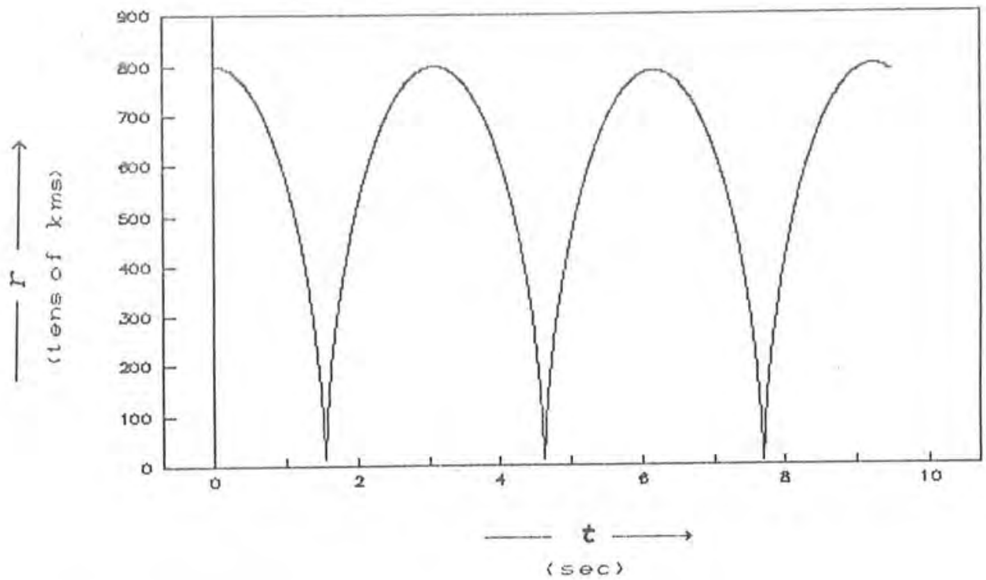

Figure 4.1. The motion of a proton in the field of a pulsar, initially at a distance of 8000 km, and $\theta = \pi/4$ and $\varphi = 0$.

a) A plot of the radial distance with time. The proton initially falls towards the neutron star and goes as near as 146 km, from where it is pushed to a distance of 7986 km; it turns again and this time its minimum distance is 112 km, the maximum being 7888 km. The proton completes this revolution in 6 secs. In successive revolutions it comes closer.

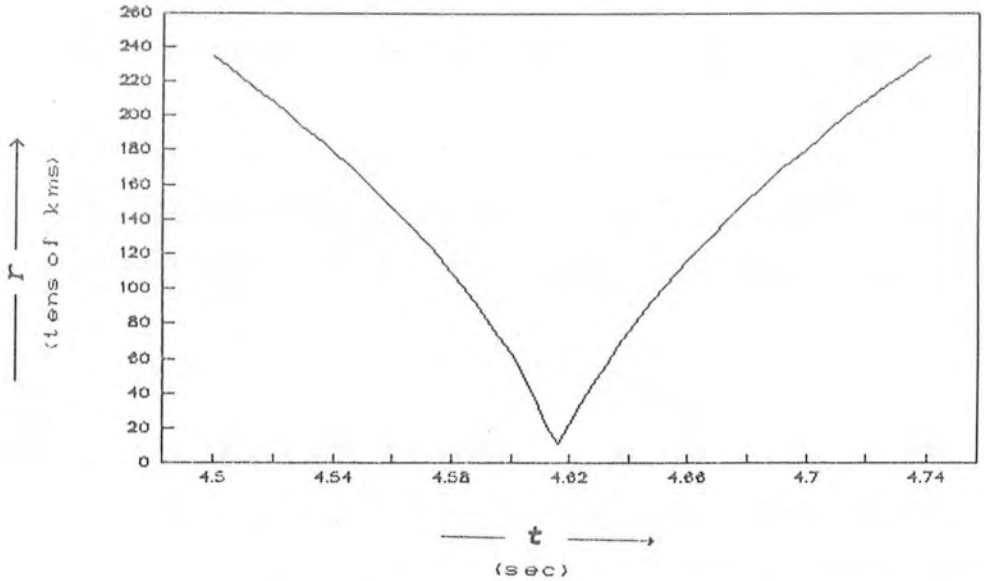

b) The previous graph in the time interval between 1.4 and 1.7 secs enlarged to show that there is no 'cusp' as seems to occur in (a). The minimum distance is also seen more clearly.

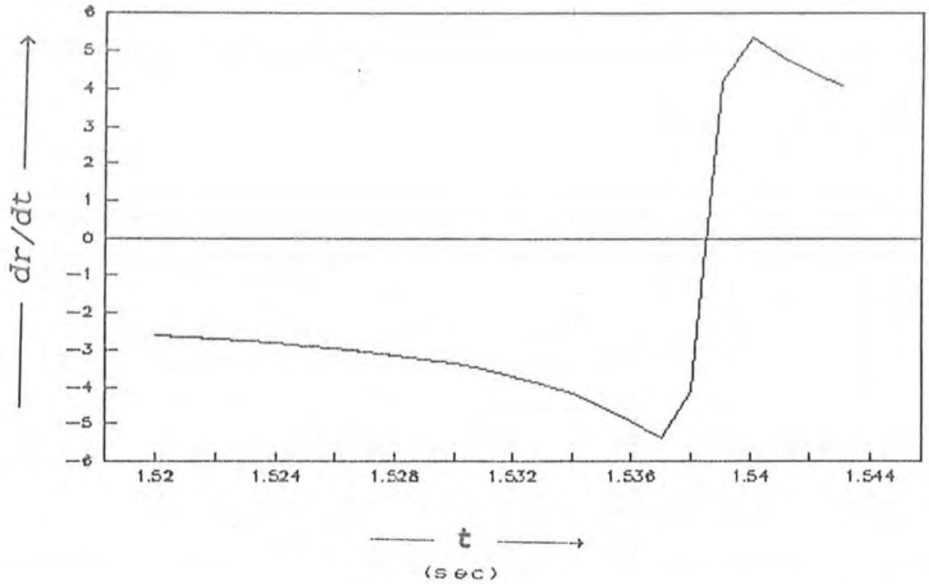

c) A plot of radial velocity with time. The proton starts with zero radial velocity which reaches its maximum when the particle is closest to the star; it again slows down and becomes zero before the particle turns around. The 'kinks' at 1.537, 1.538 and 1.539 secs disappear on expansion.

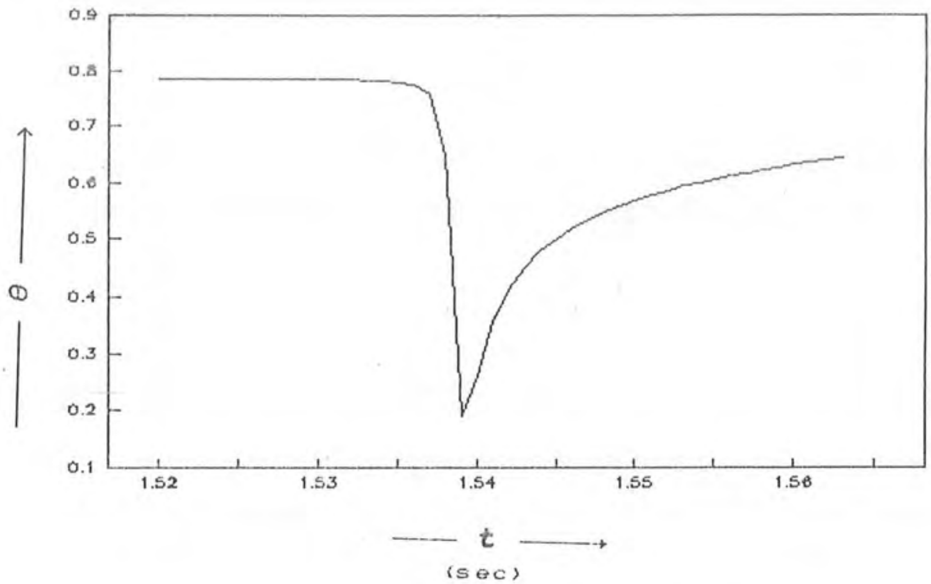

d) A plot of the polar angle with time. θ, starting from $\pi/4$ (.7854 rads), remains constant for some time and then falls to .19 rads when the particle comes nearest to the star; afterwards it increases slowly. Notice the apparent 'cusp' at 1.539 secs.

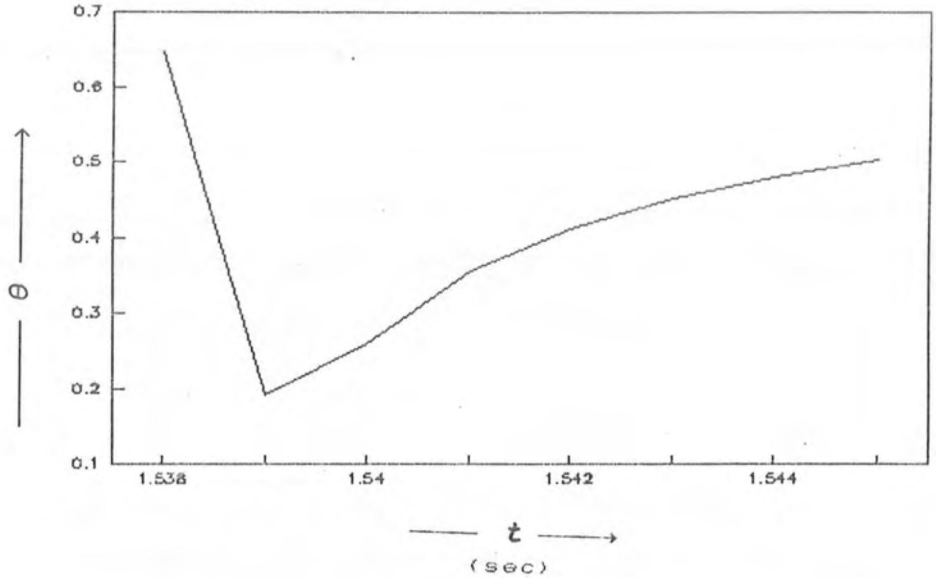

e) An enlargement of (d) in the interval when proton is nearest to the star. The 'cusp' disappears in the enlarged plot but still looks like a 'kink'. On further enlargement the 'kink' is smoothed out.

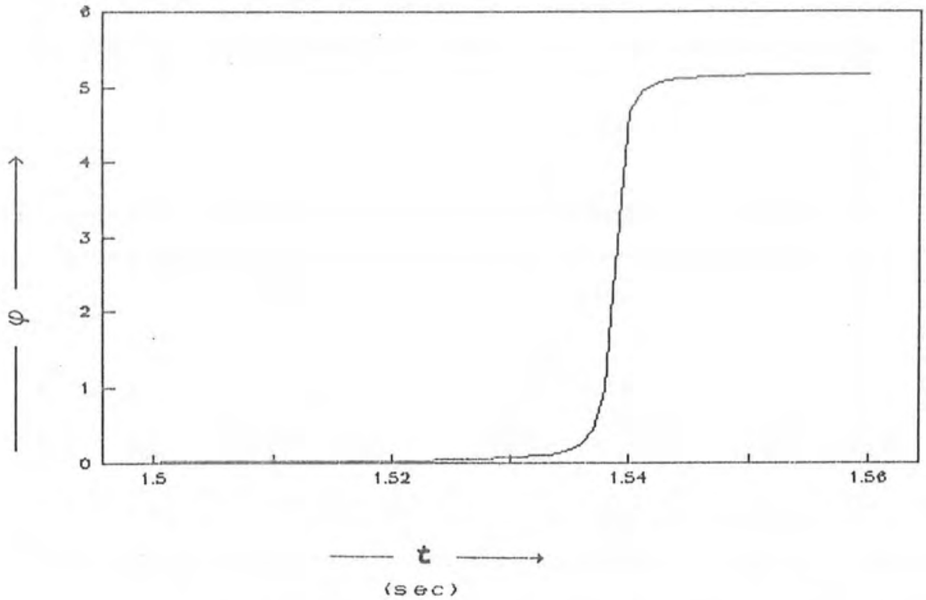

f) A plot of the azimuthal angle. Angle φ starts from zero, first increases slowly until the proton comes nearest to the star where it goes to 5.17 rads and then again goes outwards at nearly constant azimuthal angle.

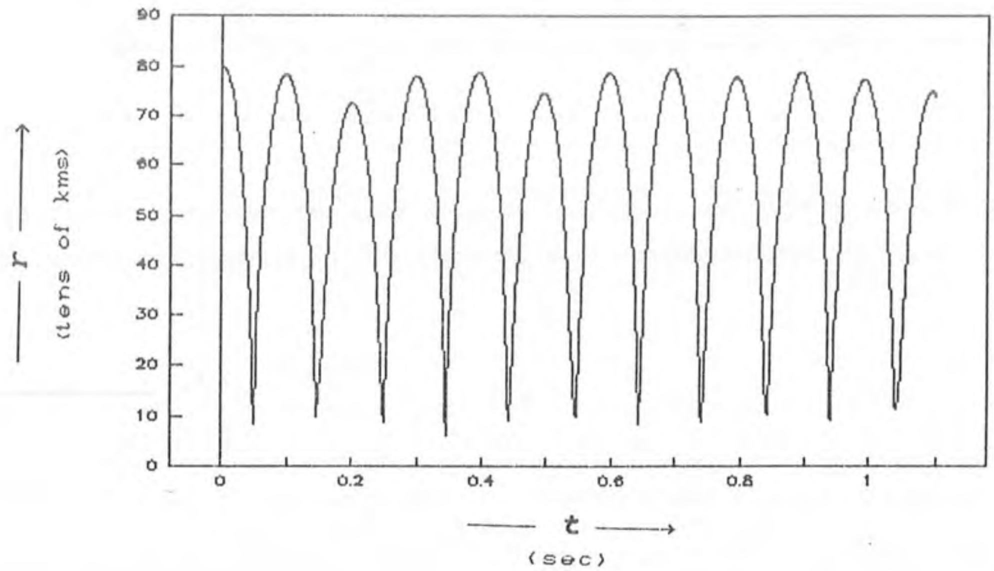

Figure 4.2. a) A plot of the radial distance with time for a proton starting from a distance of 800 km. It orbits around the neutron star in a highly elliptical orbit. It comes as near as 83 km to the star.

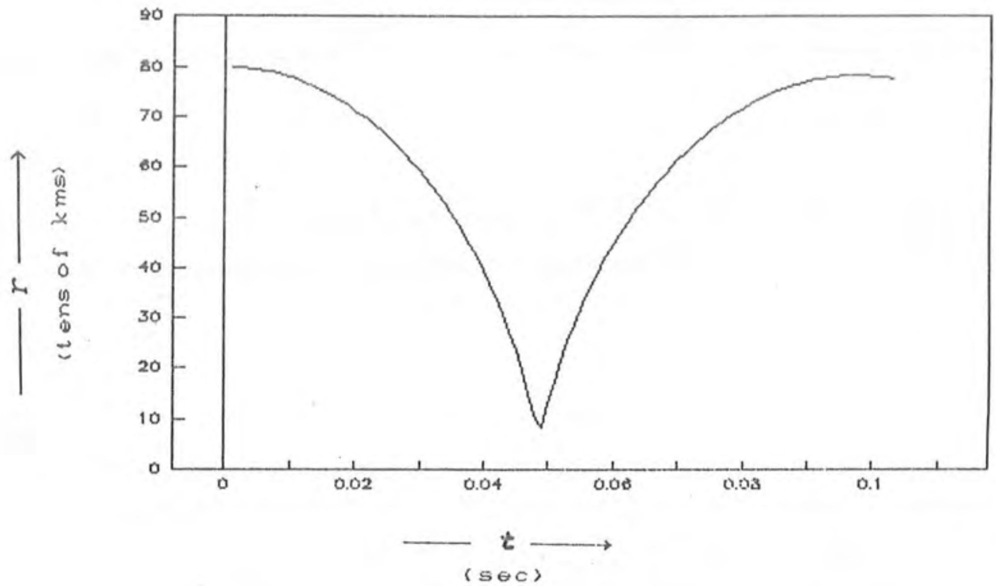

b) Enlargement of (a), when the particle first comes closest to the star. Notice that the cusp is totally smoothed out and the minimum distance is more apparent.

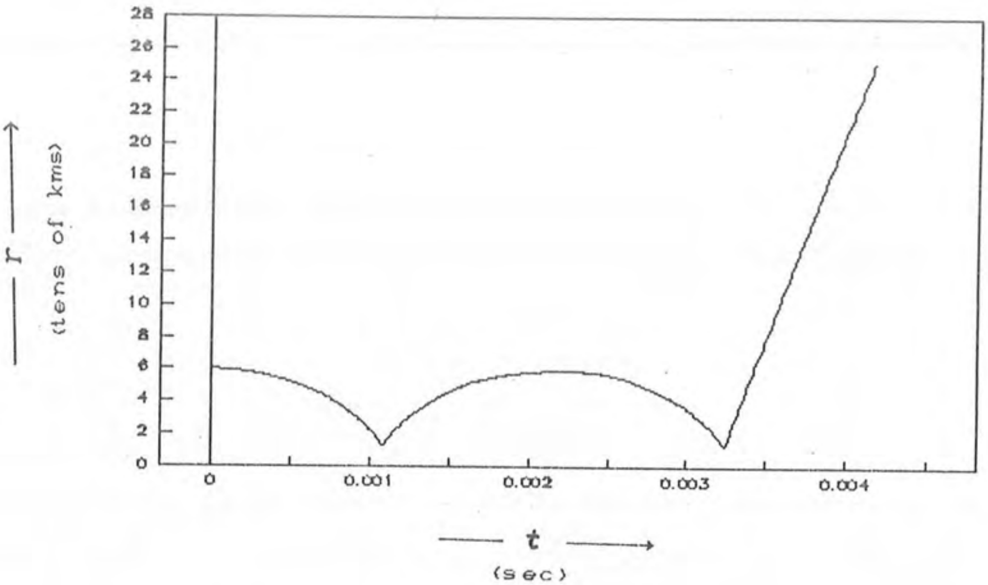

Figure 4.3. A plot of the radial distance versus time for a proton starting from a distance of 60 km. It shoots out before completing its first revolution. Its closest distance to the star is 12.88 km. Notice that if we consider a neutron star of, say, 20 km size, the particle would have been inside the star at its closest distance.

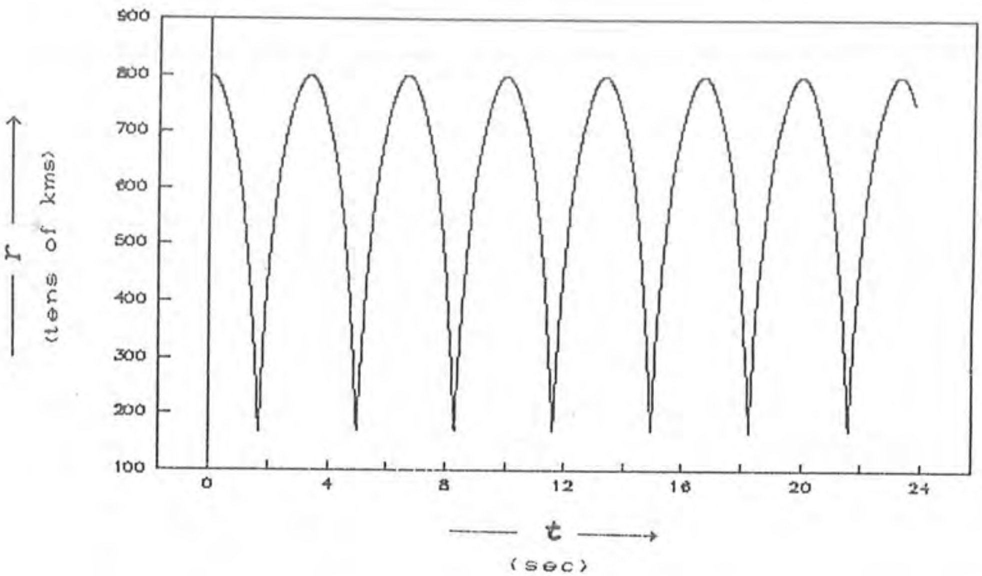

Figure 4.4. The motion of an electron in the field of a pulsar, initially at a distance of 8000 km, and $\theta = \pi/4$ and $\varphi = 0$.

a) A plot of the radial distance with time. Electron is revolving around the star in a highly elliptical orbit. Being much lighter than proton, its minimum distance from the star is 1700 km. The first revolution takes .2 secs. (Compare it with the motion of proton at the same initial distance (Fig 4.1).)

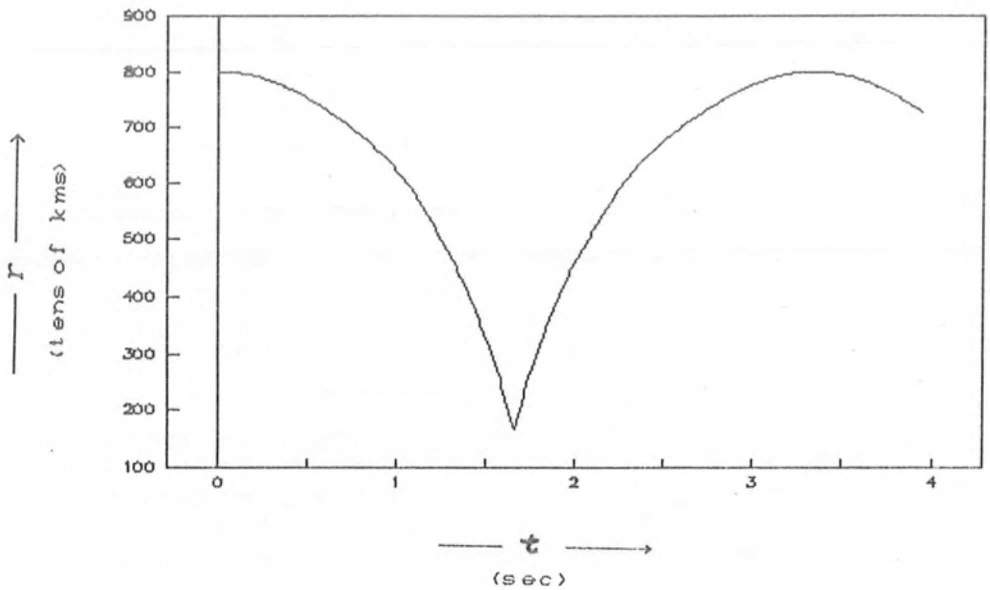

b) A part of the first oscillation of (a) enlarged. Notice that the cusp is smoothed out.

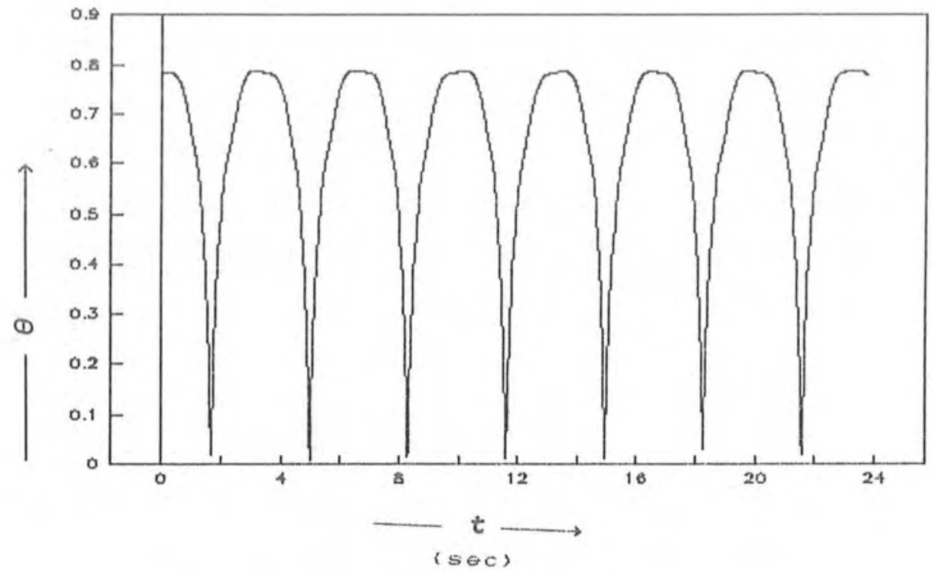

c) A plot of the polar angle with time. Starting from $\pi/4$, θ goes to .019 rads as the particle first time approaches the star; second time it is .01 and third time .015 rads.

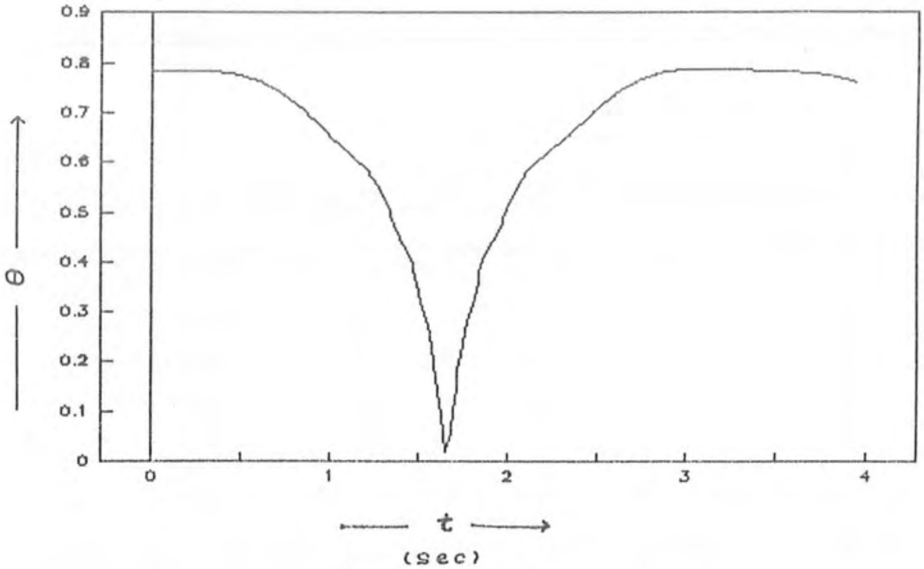

d) Enlargement of (c), when the particle first comes closest to the star. Notice that the cusp is totally smoothed out and the minimum distance is more apparent.

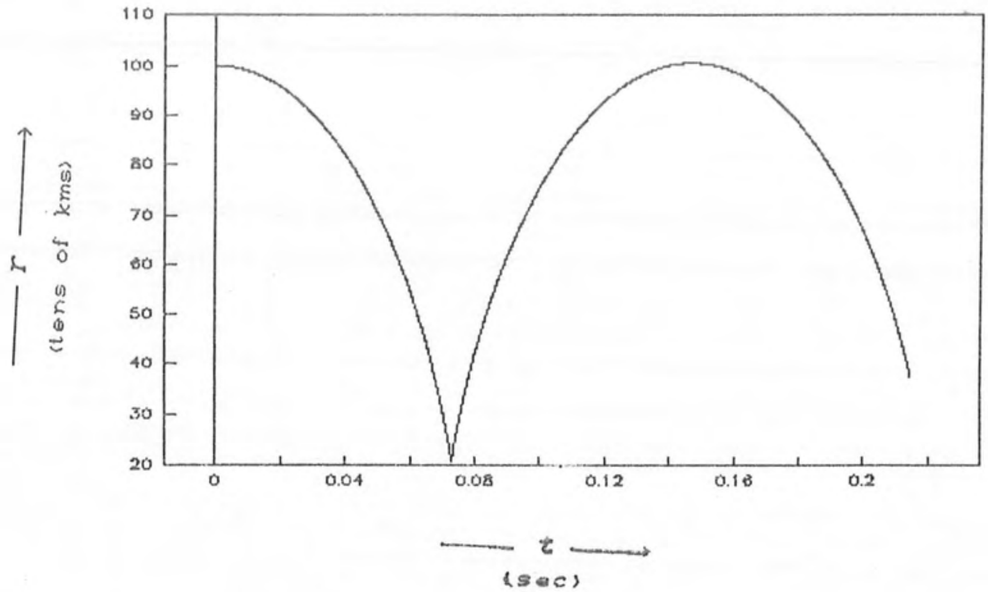

Figure 4.5. a) A plot of radial distance versus time for an electron starting at 1000 km. It goes as near as 208 km to the star.

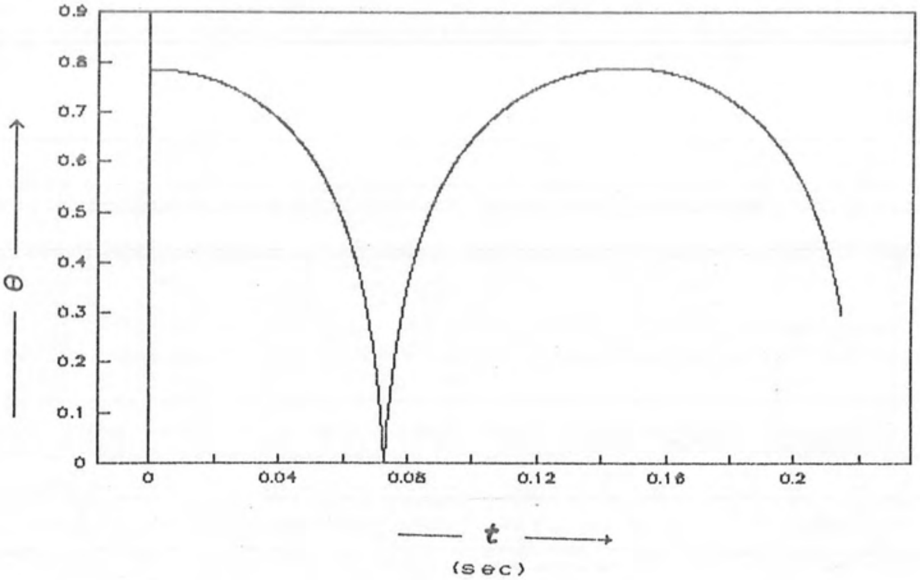

b) A plot of radial angle with time. Starting from $\pi/4$ the minimum value is .00333.

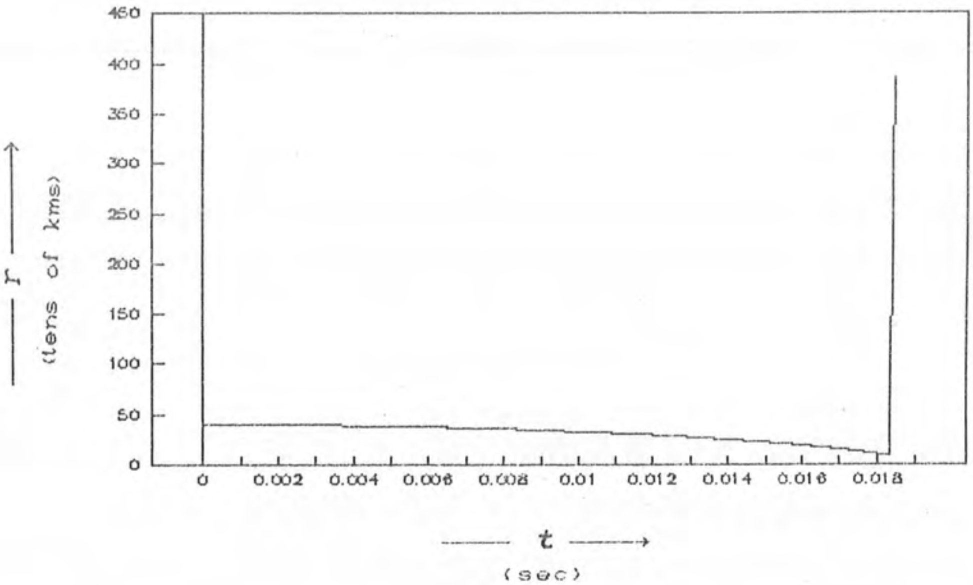

Figure 4.6. A graph showing radial distance versus time. When electrons are initially relatively close to the star, they first go towards the star and then shoot out. Starting at 400 km, electron goes to a distance of 89.54 km from where it is thrown to infinity.

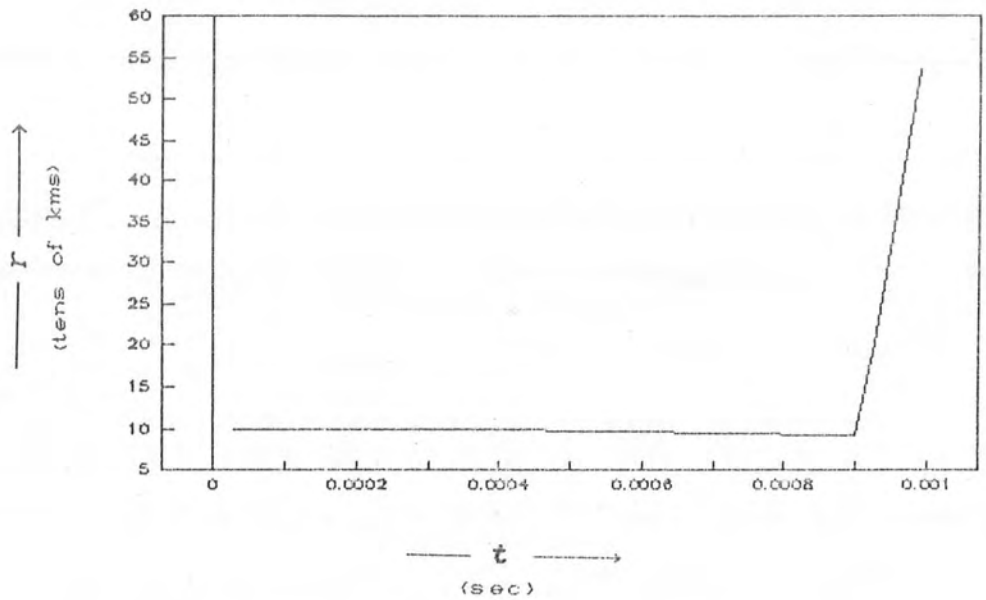

Figure 4.7. A plot of radial distance r with time for an electron. Starting at 100 km, the electron goes to about 91 km from where it shoots out.

CONCLUSION

The phenomenon of pulsar drift is one of the outstanding problems in the neutron star theory of pulsars. The problem is to explain how a supernova explosion imparts a velocity of the order of hundreds of kilometers per second to the collapsed object. Out of about 500 known pulsars, only two have been found within the supernova remnants. One of these, the Vela pulsar, is clearly off the centre of the Vela nebula.

A star of initial mass 18 - 19$M_{\odot}$, at the time of explosion is usually 9 - 10$M_{\odot}$. We do not know exactly what conditions prevail during the very short time, of the order of a second, of this explosion and implosion. For the supernova remnant to be of mass of order $M_{\odot}$, the imploded core must have densities so high that it would be nothing less than a neutron star. Also, if the magnetic flux, detected in several superdense objects, is conserved during stellar evolution, these collapsing cores must have a high magnetic field. These fields will have a dramatic influence on the less dense plasma surrounding the nascent pulsar. It is thought that the plasma would be driven in such a way that positively and negatively charged particles would move in opposite direction. This would result in the addition of angular momenta along the axis of rotating sources, which would produce an asymmetric force to cause a pulsar drift.

To fully understand the mechanism, study of the behaviour of the plasma surrounding the highly dense object with a strong dipolar magnetic field is indispensable. As a first step, within the basic framework of T. Gold's rotating neutron star model for pulsars, trajectories of charged particles in this field are calculated. It is seen that protons and electrons, at certain distances from the star, are put into stable orbits. The gravitational field pulls the particles into itself, whereas the '$\mathbf{v} \wedge \mathbf{B}$' of the Lorentz force tends to put the particle in a helical trajectory, the exact path depending on the angle between **v** and **B**. At $\theta = \pi/4$ these charges are put into an orbit which can be described as the edge of an elliptic cone, as shown in Figure 5, which in certain cases may be circular. So it appears that the

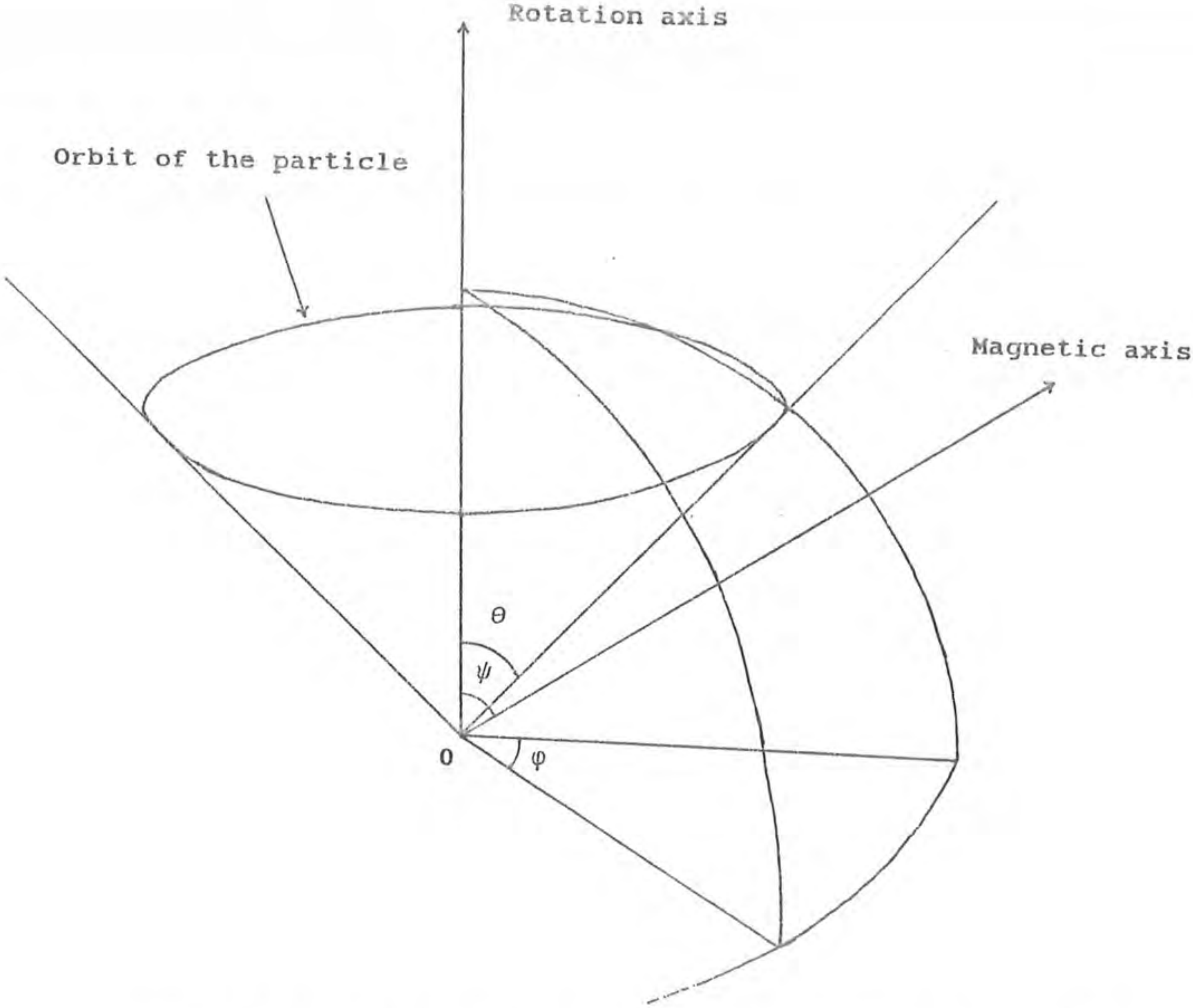

Figure 5. Particle orbiting in an elliptical orbit around a neutron star. θ is the polar angle and ψ is the angle between the rotation axis and the magnetic axis. The gravitational attraction of the star pulls the particle into itself whereas the strong magnetic field tends to put it in an orbit.

plasma, looking at it only classically, is trapped at certain regions. Clearly, $\mathbf{v} \wedge \mathbf{B}$ will be zero when $\mathbf{v}$ is parallel to $\mathbf{B}$ in which case we will only have the gravitational force.

The velocities of the particles involved are relativistic and we have strong gravitational fields (the only fields stronger than these are of black holes), therefore, there is need to incorporate relativistic effects, or rather to formulate and solve the problem general relativistically. Also, a neutral plasma surrounding the neutron star, consisting of atoms which are actually small dipoles, must be studied before any conclusions can be drawn. In this dissertation we have only conducted the first, preliminary, study.

APPENDIX

In this appendix the code for the numerical solution of Eqs. 4.17 - 4.19 is given.

```
      IMPLICIT DOUBLE PRECISION(A-H,O-Z)
*------------------------------------------------------------------
*     PROGRAM  MCFP
*     MOTION OF A CHARGED PARTICLE IN  THE FIELD OF A PULSAR
*
*     (Dated May 3rd, 1992)
*
*     This program solves the equations of motion (Eqs. 4.17
*     - 4.19) constructed in the 4th chapter of this
*     dissertation by RUNGE-KUTTA method.
*     The various constants and variables are:
*     AM1 : Mass of the neutron star
*     AM2 : Mass of the particle
*     A1  : Magnetic moment of the star
*     G   : Constant of gravitation
*     C   : Velovity of light
*     Q   : Charge of the particle
*     B   : The angle psi
*     H   : Step size
*     X   : Time
*     Y   : Radial distance
*     Z   : The angle theta
*     V   : The angle phi
*
*     (Units: cgs Gaussian )
*
*------------------------------------------------------------------

WRITE(*,*)'GIVE THE VALUES OF Y,H,N (F,OR PROTON)'
READ(*,*)Y,H,N
PI=.3141592654D+01
P2=2.*PI
Z=PI/4.0
V=0.0
B=PI/4.0
```

```
      AM1=4.0D+33
C     AM2=9.1091D-28
      AM2=1.6725D-24
      G=.6672D-07
      C=2.9979D+10
      Q=4.8030D-10
      AI=.25D+31
      X=0.0
      U=0.0
      T=0.0
      W=0.0
      F1=AM1*G
      F2=(AI*Q)/(AM2*C*C)
      WRITE(*,10)X,Y,U,Z,V,W
 10   FORMAT(1X,6E13.7)
      DO 40 I=1,N
 20   P1=H*U
      Q1=H*T
      E1=H*W
      R1=H*((-F1/(Y*Y))-((F2*DSIN(B)*W*DSIN(Z))/(Y*Y))+(Y*W*
     1W*(DSIN(Z)**2.))+(Y*T*T))
      S1=H*(((F2*2.*DCOS(B)*W*DSIN(Z))/(Y**3.))+(W*W*DSIN(Z)
     1*DCOS(Z))-((2.*U*T)/(Y)))
      D1=H*(F2*(((DSIN(B)*U)/(DSIN(Z)*(Y**4.)))-((DCOS(B)*2.
     1*T)/(DSIN(Z)*(Y**3.)))))-((2.*W*T*DCOS(Z))/(DSIN(Z)))-(
     2(2.*U*W)/(Y)))
      X1=X+.5*H
      T1=T+.5*S1
      Z1=Z+.5*Q1
      Y1=Y+.5*P1
      U1=U+.5*R1
      V1=V+.5*E1
      W1=W+.5*D1
      P2=H*U1
      Q2=H*T1
      E2=H*W1
      R2=H*((-F1/(Y1*Y1))-((F2*DSIN(B)*W1*DSIN(Z1))/(Y1*Y1))
     1+(Y1*W1*W1*(DSIN(Z1)**2.))+(Y1*T1*T1))
      S2=H*(((F2*2.*DCOS(B)*W1*DSIN(Z1))/(Y1**3.))+(W1*W1*DS
     1IN(Z1)*DCOS(Z1))-((2.*U1*T1)/(Y1)))
      D2=H*(F2*(((DSIN(B)*U1)/(DSIN(Z1)*(Y1**4.)))-((DCOS(B)
     1*2.*T1)/(DSIN(Z1)*(Y1**3.)))))-((2.*W1*T1*DCOS(Z1))/(DS
     2IN(Z1)))-((2.*U1*W1)/(Y1)))
      X2=X+.5*H
      T2=T+.5*S2
      Z2=Z+.5*Q2
      Y2=Y+.5*P2
      U2=U+.5*R2
      V2=V+.5*E2
      W2=W+.5*D2
      P3=H*U2
```

```
      Q3=H*T2
      E3=H*W2
      R3=H*((-F1/(Y2*Y2))-((F2*DSIN(B)*W2*DSIN(Z2))/(Y2*Y2))
     1+(Y2*W2*W2*(DSIN(Z2)**2.))+(Y2*T2*T2))
      S3=H*(((F2*2.*DCOS(B)*W2*DSIN(Z2))/(Y2**3.))+(W2*W2*DS
     1IN(Z2)*DCOS(Z2))-((2.*U2*T2)/(Y2)))
      D3=H*(F2*(((DSIN(B)*U2)/(DSIN(Z2)*(Y2**4.)))-((DCOS(B)
     1*2.*T2)/(DSIN(Z2)*(Y2**3.))))-((2.*W2*T2*DCOS(Z2))/(DS
     2IN(Z2)))-((2.*U2*W2)/(Y2)))
      X3=X+H
      T3=T+S3
      Z3=Z+Q3
      Y3=Y+P3
      U3=U+R3
      V3=V+E3
      W3=W+D3
      P4=H*U3
      Q4=H*T3
      E4=H*W3
      R4=H*((-F1/(Y3*Y3))-((F2*DSIN(B)*W3*DSIN(Z3))/(Y3*Y3))
     1+(Y3*W3*W3*(DSIN(Z3)**2.))+(Y3*T3*T3))
      S4=H*(((F2*2.*DCOS(B)*W3*DSIN(Z3))/(Y3**3.))+(W3*W3*DS
     1IN(Z3)*DCOS(Z3))-((2.*U3*T3)/(Y3)))
      D4=H*(F2*(((DSIN(B)*U3)/(DSIN(Z3)*(Y3**4.)))-((DCOS(B)
     1*2.*T3)/(DSIN(Z3)*(Y3**3.))))-((2.*W3*T3*DCOS(Z3))/(DS
     2IN(Z3)))-((2.*U3*W3)/(Y3)))
      X=X+H
      Y=Y+(P1+2.0*(P2+P3)+P4)/6.0
      T=T+(S1+2.0*(S2+S3)+S4)/6.0
      U=U+(R1+2.0*(R2+R3)+R4)/6.0
      Z=Z+(Q1+2.0*(Q2+Q3)+Q4)/6.0
      V=V+(E1+2.0*(E2+E3)+E4)/6.0
      W=W+(D1+2.0*(D2+D3)+D4)/6.0
      AV=DABS(V)
      WRITE(*,30)X,Y,U,Z,AV,W
30    FORMAT(1X,6E13.7)
40    CONTINUE
      STOP
      END
```

LITERATURE CITED

1. J.P.Cox and R.T.Giuli, *Principles of Stellar Structure*, Gordon and Breach, New York (1968).
2. M.Schwarzschild, *Structure and Evolution of the Stars*, Dover, New York (1965).
3. R.L.Bowers and T.Deeming, *Astrophysics I*, Jones and Bartlett, Boston (1984).
4. L.Z.Fang and R.Ruffini, *Basic Concepts in Relativistic Astrophysics*, World Scientific, Singapore (1983).
5. W. Baade and F. Zwicky, *Proc. Nat. Acad. Sci.*, **20**(1934)254.
6. R.N.Manchester and J.H.Taylor, *Pulsars*, W.H.Freeman, San Francisco (1977).
7. C.W.Misner, K.S.Thorne and J.A.Wheeler, *Gravitation*, W.H.Freeman, San Francisco (1973).
8. E.Böhm-Vitense, *Introduction to Stellar Astrophysics*, Cambridge University Press (1991).
9. S.W.Hawking, *A Brief History of Time*, Bantam, London

(1989).

10.F.Pacini, *Nature*, **216**(1967)567.

11.T.Gold, *Nature*,**218**(1968)731.

12.J.A.Wheeler, *Ann. Rev. Astron. Astrophys.*,**4**(1966)393.

13.R.Ruffini,*Physics and Contemporary Needs Vol.1*, ed. Riazuddin, Plenum Press,New York (1976).

14.M.Rafique, *M.Phil Dissertation*, Quaid-i-Azam University, Islamabad (1981).

15.A.Qadir, R.Ruffini and L.Violini, *Lett. Nuovo Cimento*, **27**(1980)381.

16.A.Qadir and J.Qamar, *Proc. 3rd Marcel Grossmann Meeting in General Relativity*, ed. HU Ning, North Holland and Science Press (1983); J. Qamar, *Ph.D. Thesis*, Quaid-i-Azam University, Islamabad (1983); S.M.Mahajan, A.Qadir and P.M.Valanju, *Nuovo Cimento* B, **65**(1981)40.

17.M.A.Abramowicz, "Centrifugal force: a few surprises", Preprint from International Centre for Theoretical Physics, Trieste.

18.A.Qadir and M.Rafique, KEXUE TONGBAO,**9**(1983)543; A.Qadir and M.Akbar, *Nuovo Cimento* B, **106**(1991)1011.

19.A.Qadir and M.Rafique, *Chinese Phys. Lett.*,**3**(1986)189.

20.A.Qadir and M.Rafique, *Proc. 4rd Marcel Grossmann*

Meeting in General Relativity, ed. R.Ruffini, Elsevier North Holland (1987); M.Rafique, *Ph.D. Thesis*, Quaid-i-Azam University, Islamabad (1985).

21.A.Qadir, M.Rafique and A.W.Siddiqui, *Chinese Phys. Lett.*,**4**(1987)177.

22.L.Z.Fang, A.Qadir and R.Ruffini, *Physics and Contemporary Needs Vol.5*, eds. Riazuddin and A.Qadir, Plenum Press, New York (1983).

23.H.Gursky and R.Ruffini eds.,*Neutron Stars, Black Holes and Binary X-Ray Sources*, D.Reidel, Dordrecht (1975).

24.A.Qadir, *Chinese Phys. Lett.*,**4**(1987)289.

25.F.Chorlton, *Textbook Of Dynamics*, Van Nostrand Reinhold, London (1973).

26.J.R.Reitz, F.J.Milford and R.W.Christy, *Foundations of Electromagnetic Theory*, Addison-Wesley, Philippines (1979).

27.A.Qadir, *Relativity: An Introduction to the Special Theory*, World Scientific, Singapore (1989).